2011

THE ROLE OF RETINOIC ACID RECEPTOR-RELATED ORPHAN RECEPTOR ALPHA IN CHONDROCYTE DIFFERENTIATION

Ryan Isaac Mark Perlus

THE ROLE OF RETINOIC ACID RECEPTOR-RELATED ORPHAN RECEPTOR ALPHA IN CHONDROCYTE DIFFERENTIATION

(Spine Title: The Role of RORα in Chondrocyte Differentiation)
(Thesis Format: Monograph)

By

Ryan Isaac Mark Perlus

Graduate Program in Physiology

A thesis submitted in partial fulfillment of the requirements for the degree of Master of Science

School of Graduate and Postdoctoral Studies
The University of Western Ontario
London, Ontario, Canada

CERTIFICATE OF EXAMINATION

Supervisors

Dr. Frank Beier (primary supervisor)

Dr. Nathalie Bérubé (co-supervisor)

Supervisory Committee

Dr. Dean Betts (GSR)

Dr. Daniel Hardy

Examiners

Dr. Tim Regnault

Dr. Rommel Tirona

Dr. Fred Possmyer

The thesis by

Ryan Isaac Mark Perlus

entitled:

The Role of Retinoic Acid Receptor-Related Orphan Receptor Alpha in Cartilage Development

is accepted in partial fulfillment of the
requirements for the degree of

Masters of Science

Date_____

Chair of the Thesis Examination Board

ABSTRACT

Endochondral bone formation is regulated by transcription factors and signaling molecules. The retinoic acid receptor-related orphan receptor alpha, RORα, is involved in tissue differentiation. RORα gene expression is upregulated during chondrocyte hypertrophy. Cholesterol, a RORα ligand, promotes chondrocyte hypertrophy and stimulates expression of lipid metabolism genes. My objective was to examine the role of RORα during chondrocyte differentiation and in the regulation of lipid metabolism genes.

Treatment of organ cultures with T0901317, a RORα inverse agonist, resulted in growth impairment, decreased hypertrophic zone length and delayed chondrocyte cell cycle exit. In micromass culture T0901317 treatment reduced chondrocyte differentiation and expression of hypertrophic differentiation markers. Lpl, a putative target of RORα, showed decreased expression upon T0901317 treatment *in vitro*. RORα overexpression in ATDC5 cells decreased *Lpl* expression.

Overall, T0901317 treatment affects chondrocyte hypertrophy. This suggests that RORα is important for chondrocyte hypertrophy, potentially through control of lipid metabolism genes.

KEYWORDS: Chondrocytes, chondrocyte differentiation, chondrocyte hypertrophy, micromass culture, RORα, lipid metabolism

ACKNOWLEDGEMENTS

First off I'd like to thank all members of the Beier lab. Others comment about the large quantity of people in the lab however, I am thankful for being surrounded by such a diverse, intelligent, and selfless group of peers. Things might be a bit fast paced and hectic at times, however, I truly believe I would not be where I am without you all. Two years ago I didn't even know what a molecular mechanism was. Thanks to you, the transition from kinesiology to molecular biology was relatively smooth. I am not going to discuss how each of you have been instrumental in my academic success, but know that each one of you holds a special place in my heart and I will never forget the experiences we have shared throughout the past two years. I would also like to thank many members of the Seguin lab and other skeletal biology labs on LG. I couldn't have asked for better neighbours.

A special appreciation is due to my supervisor, Dr. Frank Beier. The hands off approach you've adopted allowed me to develop my own hypotheses and work independently. Your open door policy always provided me a place to go when advice was needed and to ensure my progress was on the right track. Over the years, you've instilled many positive values upon your students. You've successfully created a fun and relaxed work environment yet ensured that it is place ideal for optimal productivity.

I came to LG with aspirations of receiving a Masters degree and am leaving with what is now my best friend. SEIU, words do not describe how much you've inspired me throughout the past two years. Your constant care for others, hard work ethic, and positive outlook on life has influenced me greatly. I admire how successful you've been and continue to be in all aspects of life and I am grateful that we've built an indestructible friendship.

Lastly, I'd like to thank my family for their infinite wisdom and endless support. No matter what, you have always been in my corner. You have supported and guided me through everything I have faced and are always there to encourage me to succeed in my endeavors.

TABLE OF CONTENTS

LIST OF FIGURES

LIST OF APPENDICES

LIST OF ABBREVIATIONS

ALP	Alkaline Phosphatase
Atrx	Alpha Thalassemia Mental Retardation, X-linked
BCA	Bicinchoninic Acid
BSP	Bone Sialoprotein
CD	Campomelic Dysplasia
ChIP	Chromatin Immunoprecipitation
Col10a1	Collagen, Type X, Alpha 1
Col2a1	Collagen, Type II, Alpha 1
DBD	DNA Binding Domain
DMEM	Dulbecco's Modified Eagle Medium
DMSO	Dimethyl Sulfoxide
EC	Embryonal Carcinoma
Fabp3	Fatty Acid Binding Protein 3
Fabp4	Fatty Acid Binding Protein 4
FGF21	Fibroblast Growth Factor 21
Gapdh	Glyceraldehyde 3-Phosphate Dehydrogenase
Gsk3b	Glycogen synthase Kinase 3 Beta
HDL	High Density Lipoprotein
HDL-C	High Density Lipoprotein-Cholesterol
Ihh	Indian Hedgehog
LBD	Ligand Binding Domain

Lipg	Endothelial Lipase
Lpl	Lipoprotein Lipase
LXR	Liver X Receptor
Mmp13	Matrix Metalloproteinase 13
Mmp9	Matrix Metalloproteinase 9
OA	Osteoarthritis
PBS	Phosphate Buffered Saline
PCNA	Proliferating Cell Nuclear Antigen
Pdk4	Pyruvate Dehydrogenase Kinase Isozyme 4
PPAR	Peroxisome Proliferator-Activated Receptor
PPRE	Peroxisome Proliferator Response Element
PTHrP	Parathyroid Hormone-Related Protein
qPCR	Real-Time PCR
RA	Retinoic Acid
Rac1	Ras-related C3 Botulinum Toxin Substrate 1
RAR	Retinoic Acid Receptor
RE	Response Element
RIPA	Radioimmunoprecipitation
ROR	Retinoic Acid Receptor-Related Orphan Receptor
RORα	Retinoic Acid Receptor-Related Orphan Receptor Alpha
RORβ	Retinoic Acid Receptor-Related Orphan Receptor Beta
RORγ	Retinoic Acid Receptor-Related Orphan Receptor Gamma

Runx2	Runt Domain Transcriptional Activator
RXR	Retinoid X Receptor
Sg	Staggerer
Sox	SRY-box 9
SRY	Sex Determining Region Y
TR	Thyroid Hormone Receptor
VDR	Vitamin D Receptor
VEGF	Vascular Endothelial Growth Factor
α	Alpha
β	Beta
γ	Gamma

CHAPTER ONE

LITERATURE REVIEW

1.1 Biology of Skeletal Development

The skeletal system serves as the basis for all human locomotion. Skeletal development is a tightly regulated process and its disruption can lead to numerous skeletal malformations and diseases including chondrodysplasias and osteoarthritis. Bone formation can take place through two distinct mechanisms; intramembranous ossification and endochondral ossification. Intramembranous ossification is described by the formation of bone directly from mesenchymal precursor cells (Opperman 2000; Street, Bao et al. 2002; Kronenberg 2003). This process occurs in bones such as the flat bones of the skull and the mandible. Endochondral ossification, on the other hand, involves bone development through a cartilage intermediate.

1.1.1 Endochondral Ossification

The majority of our bones are formed through the process of endochondral ossification. Here, mature bone is formed from a cartilage intermediate that is subsequently replaced by bone tissue and marrow (Stanton, Underhill et al. 2003; Beier 2005). This process is tightly regulated by a vast number of transcription factors and signaling molecules.

1.1.2 Chondrogenesis

Endochondral ossification begins with the formation of mesenchymal condensations; clusters of cells that adhere through the expressions of adhesion molecules. The cells in the center of the condensations undergo chondrogenic differentiation (Kronenberg 2003). Specifically, these central cells convert into pre-chondrocytes and begin to express early cartilage markers while simultaneously, turning off expression of mesenchymal and condensation markers (Lefebvre, Li et al. 1998).

While the cells in the middle of the aggregates differentiate into chondrocytes, the cells in the periphery flatten and elongate to become what is known as the perichondrium (Figure 1.1) (Kronenberg 2003). In humans, these condensations can be found at 6.5 weeks of gestations and in mice at 10.5 days of embryonic development (Ballock and O'Keefe 2003).

1.1.3 Chondrocyte Differentiation

Once committed to the chondrogenic pathway, chondrocytes undergo a variety of further maturation steps involving proliferation and hypertrophy in the spatial context of the growth plate. Growth plates are located at either end of the bone and control longitudinal growth. The growth plate is organized into three well-defined zones; resting, proliferative, and hypertrophic. From the end of the bone to the center the first zone of the growth plate is known as the resting zone (Figure 1.2). This zone can be classified according to its cell morphology where chondrocytes are small, round, and surrounded by a vast quantity of extracellular matrix rich in type II collagen, proteoglycans such as aggrecan and cross-linking proteins (Beier 2005). Next to the resting zone is the proliferative zone which is characterized by chondrocytes that are discoidal in shape and display a columnar organization (Figure 1.2) (Beier 2005). These cells undergo rapid cell division. Once division is completed, they exit the cell cycle and become prehypertrophic as they increase their size compared to their proliferative precursors (Hunziker 1994); however, they are still smaller in volume compared to the next zone and final portion of the growth plate, the hypertrophic zone.

Figure 1.1 Overview of Chondrogenesis

Mesenchymal cells begin to form condensations and eventually undergo chondrogenic differentiation. Cells in the middle of the aggregates begin to express cartilage specific markers while cells in the periphery flatten and elongate to form the perichondrium. Chondrocytes then proliferate and differentiate to form the cartilage anlagen.

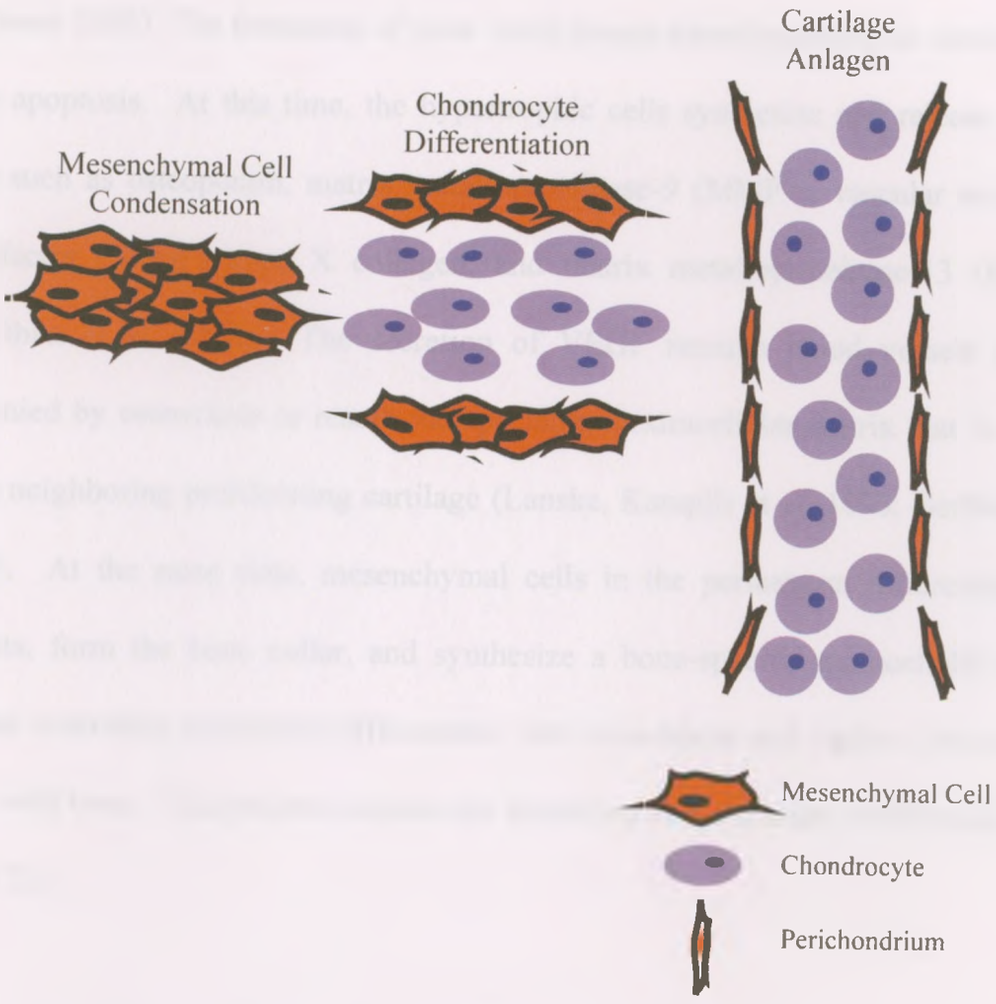
Cartilage
Anlagen
Chondrocyte
Differentiation
Mesenchymal Cell
Condensation
Mesenchymal Cell
Chondrocyte
Perichondrium

1.1.4 Hypertrophic Chondrocytes and Mineralization

Hypertrophic chondrocytes are responsible for many crucial actions in endochondral ossification and are considered to be a master regulator of bone growth. Chondrocytes in the hypertrophic zone are much larger in volume and have a cuboidal shape (Beier 2005). The formation of bone itself occurs when hypertrophic chondrocytes undergo apoptosis. At this time, the hypertrophic cells synthesize and release specific markers such as osteopontin, matrix metalloproteinase-9 (MMP9), vascular endothelial growth factor (VEGF), type X collagen, and matrix metalloproteinase-13 (MMP13) (Hojo, Ohba et al. 2010). The secretion of VEGF recruits blood vessels that are accompanied by osteoclasts to resorb the specialized extracellular matrix that is distinct from the neighboring proliferating cartilage (Lanske, Karaplis et al. 1996; Gerber, Vu et al. 1999). At the same time, mesenchymal cells in the periosteum differentiate into osteoblasts, form the bone collar, and synthesize a bone-specific extracellular matrix. Additional osteoblast precursors differentiate into osteoblasts and replace the cartilage template with bone. This process initiates the formation of the primary ossification center (Figure 1.2).

1.2 Molecular Control of Chondrocyte Differentiation

1.2.1 Sex Determining Region Y Box Family (Sox) 5, 6, 9

Chondrogenesis involves a complex and tightly regulated series of events that is controlled by variety of transcription factors. The members of the SRY (sex determining region Y) box family (Sox), specifically Sox9, L-Sox5 and Sox6, play

Figure 1.2 Endochondral Ossification

Chondrocytes present in the cartilage anlagen further differentiate into three distinct zones; resting, proliferative, and hypertrophic. Before hypertrophic chondrocytes undergo apoptosis, these cells synthesize specific matrix components and growth factors that promote vascular invasion. The appearance of the vasculature is accompanied by osteoclasts to resorb bone. The cartilage matrix left behind by hypertrophic chondrocytes that under apoptosis provides a scaffold for osteoblasts to synthesize a bone specific matrix, forming the Primary Ossification center. At this time, mesenchymal cells in the periosteum differentiate into osteoblasts to form the bone collar. In the distal ends of the bone, chondrocytes undergo terminal chondrocyte differentiation, attract blood vessels and initiate the secondary ossification center.

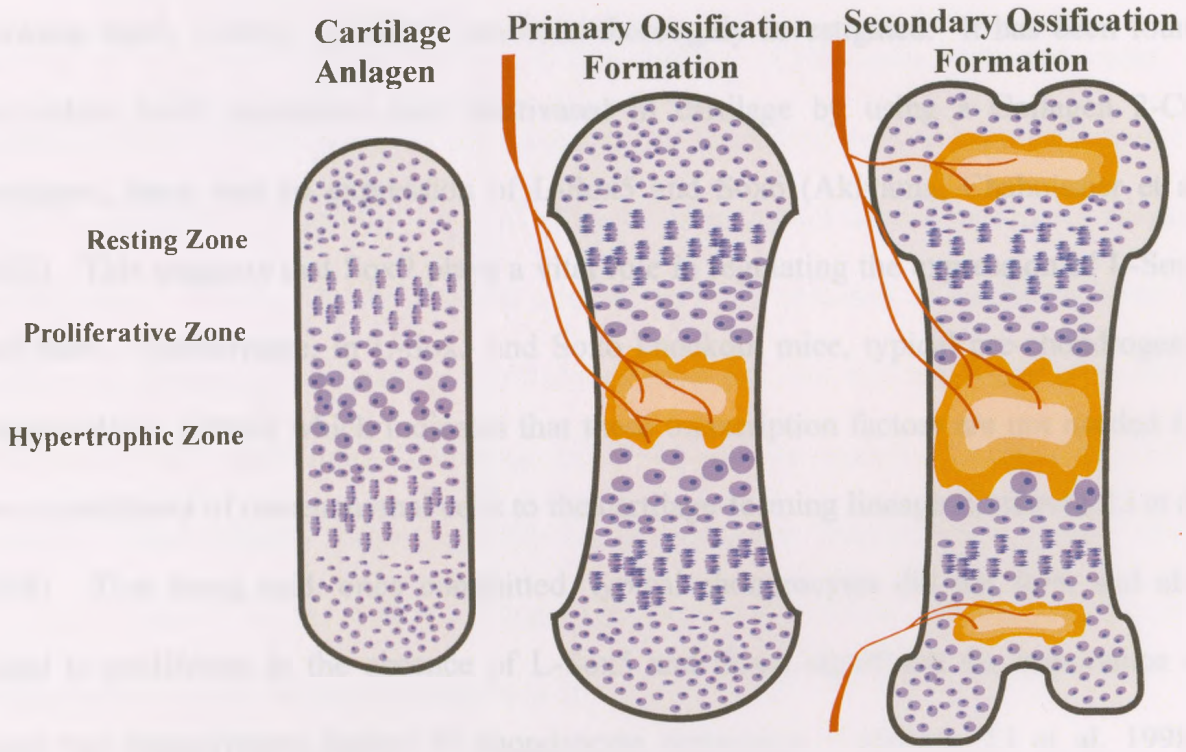
Cartilage Anlagen
Primary Ossification Formation
Secondary Ossification Formation
Resting Zone
Proliferative Zone
Hypertrophic Zone

dominant roles in this process (Lefebvre, Li et al. 1998). The role of Sox9 in chondrogenesis was originally recognized through mutations in the gene that caused a severe skeletal disease called Campomelic Dysplasia (CD) in humans (Foster 1995). It has subsequently been found that inactivation of Sox9 in limb bud mesenchyme results in the complete absence of condensations and consequently, formation of the cartilage anlagen (Akiyama, Chaboissier et al. 2002). Furthermore, the relationship and interaction between Sox9, L-Sox5, and Sox6 has been thoroughly investigated. It has been found that when Sox9 expression was inactivated in cartilage by using a Collagen 2-Cre transgene, there was no expression of L-Sox5 and Sox6 (Akiyama, Chaboissier et al. 2002). This suggests that Sox9 plays a vital role in regulating the expression of L-Sox5 and Sox6. Furthermore, in L-Sox5 and Sox6 knockout mice, typical pre-chondrogenic condensations formed which indicates that these transcription factors are not needed for the commitment of mesenchymal cells to the cartilage-forming lineage (Lefebvre, Li et al. 1998). That being said, once committed, typical chondrocytes did not form and also failed to proliferate in the absence of L-Sox5 and Sox6, signifying the importance of these two transcription factors in chondrocyte maturation (Lefebvre, Li et al. 1998). Upon interaction, Sox9, L-Sox5 and Sox6 cooperate with each other to stimulate the expression of type II collagen and other cartilage markers such as aggrecan (O'Keefe, Puzas et al. 1994; Zhao, Eberspaecher et al. 1997).

Type II collagen is the major extracellular matrix component of cartilage, constituting up to sixty percent of the total protein content (Ng, Wheatley et al. 1997). The collagen II protein in mouse is encoded by the *Col2a1* gene and its expression is considered to be one of the hallmarks of chondrogenesis (O'Keefe, Puzas et al. 1994; Ng, Wheatley et al. 1997; Zhao, Eberspaecher et al. 1997). It is evident that there is

coexpression and a tight regulation of both the *Sox9* and *Col2a1*genes and Sox9 protein in the differentiation of chondrocytes (Ng, Wheatley et al. 1997). Both *Sox9* and *Col2a1* are highly expressed in cartilaginous tissue until chondrocytes undergo hypertrophy and mineralization occurs (Ng, Wheatley et al. 1997).

1.2.1 p57-kip2

Cell proliferation is controlled by the cell cycle machinery and in particular by the activity of cyclin-dependent kinases (Beier 2005). Cell cycle exit and onset of prehypertrophic differentiation of chondrocytes are controlled by p57, a cyclin dependent kinase inhibitor that functions to inhibit all G1/S phase cyclin dependent kinases (Zhang, Liegeois et al. 1997). In the skeletal system, p57 is expressed at moderate levels in resting chondrocytes, low levels in proliferating chondrocytes, and very high levels in the prehypertrophic zone (Zhang, Liegeois et al. 1997). *In vivo* analysis has showed that p57 knockout mice display shorter, thicker bones that have reduced hypertrophic zones (Zhang, Liegeois et al. 1997). Thus, p57 null mice show delayed chondrocyte differentiation and postponed cell cycle exit.

1.2.2 The Indian Hedgehog/Parathyroid Hormone-Related Protein Negative Feedback Loop

Indian hedgehog (Ihh) is a member of the hedgehog family of secreted ligands and is synthesized by prehypertrophic and hypertrophic chondrocytes (Kronenberg 2003). Ihh regulates the progression of the cell cycle and stimulates the expression of parathyroid hormone-related protein (PTHrP). PTHrP is a peptide that is secreted by both proliferating chondrocytes and the perichondrial cells. PTHrP signaling is required to

keep chondrocytes in the proliferative pool by inhibiting the onset of hypertrophic differentiation (St-Jacques, Hammerschmidt et al. 1999). An increase in chondrocyte hypertrophy is accompanied by an increase in Ihh/PTHrP signaling. This triggers a negative feedback loop, which ultimately prevents additional chondrocytes from exiting the cell cycle, and differentiating into hypertrophic chondrocytes thus preserving the proliferative pool (Vortkamp, Lee et al. 1996; Kobayashi, Chung et al. 2002). Subsequently, Ihh and PTHrP levels will decrease and terminal differentiation will continue. As such, the length of proliferating columns and ultimately, the growth of the cartilage growth plate is tightly regulated by the Ihh-PTHrP negative feedback loop.

1.2.3 Runx2

Runx2, formerly known as Cbfa1, is a member of the family of transcription factors containing a runt-domain. Its role in skeletal development was discovered when Runx2 knockout mice failed to form osteoblasts and therefore did not undergo ossification (Komori, Yagi et al. 1997). Runx2 is highly expressed in prehypertrophic and hypertrophic chondrocytes, perichondrial cells, and osteoblasts (Kronenberg 2003). A dominant negative form of Runx2 inhibited chondrocyte hypertrophy (Hojo, Ohba et al. 2010). Similar results were seen in Runx2 knockout mice. As such, it has been established that Runx2 induces chondrogenic differentiation and hypertrophy.

1.3 Disorders of Cartilage

1.3.1 Chondrodysplasias

Skeletal dysplasias are a group of genetic disorders characterized by severe impairment of bone growth (Yasoda, Kitamura et al. 2009). Although individually each

dysplasia is considered to be rare, together this diverse group of disorders affects a large number of individuals and causes severe morbidity and mortality (Superti-Furga, Bonafe et al. 2001). Chondrodysplasia is a subset of skeletal dysplasia caused by genetic defects affecting chondrogenesis and cartilage development (Matsui 2010). There are over 150 different forms of chondrodysplasias (Spranger 1992). These diseases are characterized by disordered cartilage development and bone formation resulting in dwarfism and poor bone quality (Schwartz and Domowicz 2002). Campomelic dysplasia (CD) is one type of chondrodysplasia that is caused by mutations in *Sox9*. The most obvious feature of CD is congenital bowing and angulation of the long bones which is often found combined with other skeletal abnormalities and defects in cartilage formation (Foster, Dominguez-Steglich et al. 1994). Another example of a chondrodysplasia is Type II Collagenopathy. This disease is a result of mutations in the gene for type II collagen (Spranger, Winterpacht et al. 1994). There are many forms of this disease and severity can vary among patients. Some might experience moderate forms of Type II Collagenopathy such as dwarfism while for others the disease may be lethal (Spranger, Winterpacht et al. 1994). There are also forms of chondrodysplasias that are a result from mutations in other collagen components such as genes encoding type IX collagen and type X collagen, to name a few (Olsen, Reginato et al. 2000).

1.3.2 Osteoarthritis

Osteoarthritis (OA), the most common joint disease, can lead to joint pain and dysfunction (Buckwalter and Martin 2006). It is found in more than a third of people over 45 years old and in more than 60% of people over the age of 65 (Buckwalter and Mankin 1998; Buckwalter, Martin et al. 2000). Symptoms of OA can vary from a

sensation of occasional joint stiffness and intermittent pain to permanent loss of motion and constant deep pain (Buckwalter and Mankin 1998; Poole 1999; Buckwalter, Martin et al. 2000). OA is characterized by joint degeneration, and may include degradation and loss of articular cartilage, remodeling and sclerosis of subchondral bone, as well as osteophyte formation (Buckwalter and Mankin 1998; Buckwalter, Martin et al. 2000). The pathophysiology of OA remains poorly understood however, as the disease appears to be caused by a combination of biological, mechanical, and genetic factors (Buckwalter and Martin 2006). The primary mechanism of cartilage degeneration however, appears to be the inability of chondrocytes to maintain a constant balance between cartilage synthesis and degradation, resulting in extracellular matrix catabolism (Aigner, Sachse et al. 2006).

During endochondral ossification, chondrocytes are extremely dynamic, but, articular chondrocytes found in synovial joints are much more static (Aigner, Kurz et al. 2002; Dreier 2010). In OA however, articular chondrocytes have been found to behave more like growth plate chondrocytes and undergo hypertrophy (Aigner, Kurz et al. 2002; Dreier 2010). When this process occurs, these articular chondrocytes begin to alter their expression profiles and act like hypertrophic chondrocytes. They begin to expression metalloproteinases and alkaline phosphatase and this alteration is thought to contribute to OA (Aigner, Kurz et al. 2002; Dreier 2010). Importantly, mouse mutants that show delayed hypertrophic differentiation are protected from surgically-induced OA (Appleton, Pitelka et al. 2007; Fu, Wang et al. 2011). Thus, any mechanisms that promote chondrocyte hypertrophy during development are potential drug targets for the treatment of OA.

1.4 Nuclear Receptors

A great number of biological responses to steroid hormones and other lipophilic substances are mediated through the interaction of these molecules with their respective intracellular nuclear receptors. There are three well defined categories of the nuclear receptor family: steroid hormone receptors, thyroid/retinoid/vitamin D receptors, and peroxisome proliferator activated receptors (Kumar and Thompson 1999). The majority of nuclear receptors, however, have not been linked with a known ligand and have consequently been identified as nuclear orphan receptors (Kumar and Thompson 1999).

1.4.1 Nuclear Receptor Structure

All members of the nuclear receptor superfamily share one major feature, a DNA binding domain (DBD) located at the amino terminal which is crucial for the recognition of specific DNA sequences and protein:protein interactions. Another highly preserved region of nuclear receptors is the ligand binding domain (LBD) located at the carboxy terminal end which is important for hormone binding, protein:protein interactions, and additional transactivation activity (Giguere 1999; Kumar and Thompson 1999). Other distinct areas of typical nuclear receptors are their hinge regions and modulator domains, both serving a specific function (Figure 1.3A). Most nuclear receptors are constitutively nuclear and often bound to DNA in the absence of their ligand (Giguere 1999).

Figure 1.3 RORα Structure and Function

A) Schematic structure of the various mouse RORα isoforms (α1 and α4). The transcription activation function 1 (AF1) domain, DNA binding domain, hinge region, ligand binding domain (LBD), and transcription activation function 2 (AF2) domain are indicated. The numbers on the right refer to the total number of amino acids in each RORα isoform. B) Mechanism of action of RORα. RORα binds as a monomer to ROREs. RORα interacts with coactivators or corepressors to enhance or suppress gene transcription.

A


AF1
DBD
Hinge
LBD
AF2
RORα1
523
RORα4
468

B

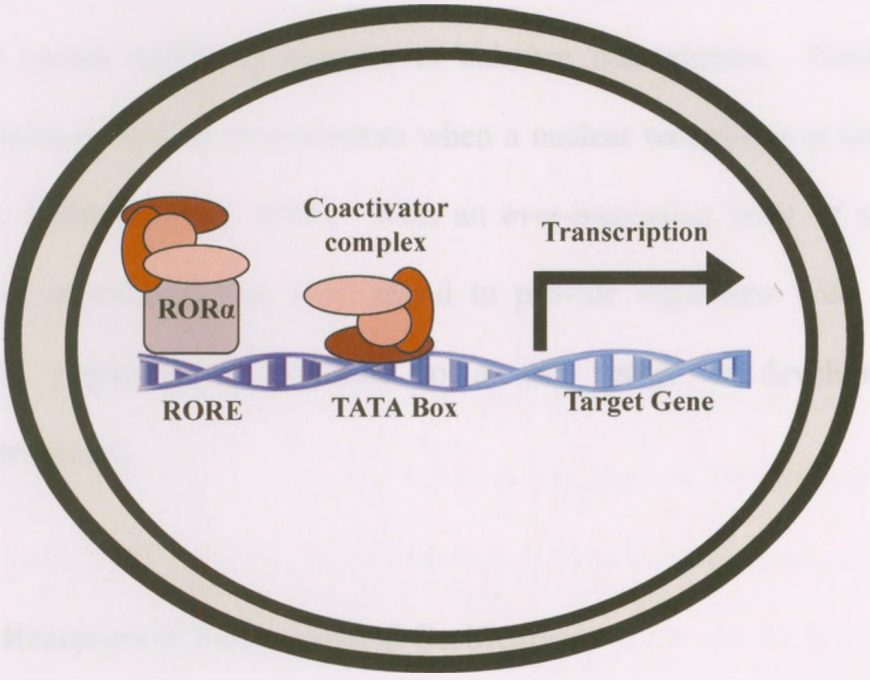
Coactivator complex
Transcription
RORα
RORE
TATA Box
Target Gene

1.4.2 Nuclear Receptor Function

All nuclear receptors function by regulating transcription, with or without a ligand. Transcriptional control can be achieved through a variety of mechanisms involving direct interaction of the receptor with specific DNA sequences, with a variety of proteins, or both (Kumar and Thompson 1999). Nuclear receptors attach to DNA binding sites called Response Elements (RE) which are short patterned DNA sequences of specific nucleotides (Figure 1.3B) (Kumar and Thompson 1999). Nuclear receptors can act as both strong activators and repressors of gene expression (Chen and Evans 1995; Horlein, Naar et al. 1995). In many instances, nuclear receptors interact with co-regulatory proteins in order to modulate transcription of their target genes (Figure 1.3B) (Giguere 1999). In the presence of a ligand, co-regulatory proteins will act as co-activators and recruit additional proteins to enhance transcription. Conversely, co-regulatory proteins behave as co-repressors when a nuclear receptor is in its unliganded form (Weston, Hoffman et al. 2003). With an ever-increasing body of research, the nuclear receptor superfamily has been found to provide organisms with a means to directly control expression in response to a wide range of developmental and physiological processes.

1.4.3 Nuclear Receptors in Endochondral Ossification

1.4.3.1 Vitamin D Receptor

Vitamin D is required for normal calcium and bone homeostasis. This hormone functions by activating its receptor, the vitamin D receptor (VDR). The VDR is ubiquitously expressed and is highly involved in the regulation of calcium absorption in

the intestine and reabsorption in the kidney (Bouillon, Carmeliet et al. 2008). Activation of the VDR relies on the binding of its ligand 1,25-dihydroxyvitamin D_3 (1,25-$(OH)_2$D) and the formation of a heterodimer with all isoforms of another nuclear receptor, the retinoid X receptor. In VDR knockout mice, there is no skeletal phenotype at birth. At weaning, however, VDR null mice are growth retarted and show multiple skeletal defects (Li, Pirro et al. 1997; Yoshizawa, Handa et al. 1997). At this age, longitudinal growth of long bones is diminished and there is disorganization of growth plates with impaired mineralization of hypertrophic chondrocytes (Li, Pirro et al. 1997; Yoshizawa, Handa et al. 1997; Erben, Soegiarto et al. 2002). The resting and proliferative chondrocytes and the expression of typical markers of chondrocyte differentiation appear normal however there is a drastic decrease in hypertrophic chondrocyte apoptosis. VDRs function to regulate bone development by inducing expression of paracrine factors such as VEGF, which leads to increased vascular invasion, and increased osteoclast number (Bouillon, Carmeliet et al. 2008).

1.4.3.2 Thyroid Hormone Receptor

Thyroid hormone receptors (TR) are located in the nucleus and act as hormone-activated transcription factors. There are a variety of isoforms of TR however, only three, TRα1, TRα2, and TRβ1, have been identified during endochondral bone growth (Bassett and Williams 2003). All three isoforms are synthesized in the resting and proliferative zones but not in the hypertrophic zone (Stevens, Hasserjian et al. 2000). Upon activation, TRs primarily form heterodimers with the retinoid X receptor but they also have the capability of forming homodimers. In mouse models using TRα knockout mice, there is an overall delay in growth plate maturation and decreased mineralization (Bassett and

Williams 2003). In TRβ null mice, growth plates appear to be narrow which is also accompanied by amplified primary and secondary ossification (Bassett, O'Shea et al. 2007). Triiodothyronine (T_3), a thyroid hormone, inhibits chondrocyte proliferation while simultaneously promoting hypertrophic chondrocyte differentiation (Miura, Tanaka et al. 2002).

1.4.3.3 Peroxisome Proliferator-Activated Receptor Gamma

There are three forms of the peroxisome proliferator-activated receptor (PPAR): PPARα, PPAR δ, and PPARγ. All PPARs form heterodimers with the retinoid X receptor and bind to peroxisome proliferator response elements (PPRE) in the promoter regions of target genes (Shao, Wang et al. 2005). PPARs are known as key regulators of many physiological processes, mainly adipogenesis and lipid metabolism. In the cartilage growth plate, while transcripts for all three forms are present, only PPARγ protein is detectable. PPARγ activation through treatment with a synthetic ligand and through a pharmacological agonist results in the blockade of T_3-induced terminal differentiation as well as increased apoptosis (Shao, Wang et al. 2005; Stanton, Li et al. 2010).

1.4.3.4 Retinoic Acid Receptor

Retinoic acid receptors (RAR) are the major receptors for retinoic acid (RA), a metabolite of vitamin A. The RAR family has three members, α, β, and γ, each with their own set of isoforms. Both RARα and RARγ are expressed throughout limb mesenchyme with RARα expression downregulated upon chondrocyte differentiation (Weston, Hoffman et al. 2003). RARγ, on the other hand, is expressed throughout chondrocyte differentiation and upregulated just prior to hypertrophy (Koyama, Golden et al. 1999). Surprisingly, in RARα, -β, and –γ knockout mice, there are no noticeable skeletal defects

(Lohnes, Kastner et al. 1993; Lufkin, Lohnes et al. 1993; Ghyselinck, Dupe et al. 1997). Despite the lack of a phenotype, there are dramatic skeletal defects in the developing limb when ectopic expression of a constitutively active RAR prevents mesenchymal condensations from undergoing chondrocyte differentiation (Weston, Rosen et al. 2000; Weston, Chandraratna et al. 2002). When mesenchymal cells that have completed chondrogenesis are treated with RAR antagonists, there is an induction of *Sox9* expression and activity (Weston, Chandraratna et al. 2002). The roles of RARs extend beyond chondrogenesis. RARs are known to be major regulators of chondrocyte hypertrophy and mineralization (Weston, Hoffman et al. 2003). Overall, a loss of retinoid signaling is accompanied by an induction of chondrogenesis and a delay in chondrocyte differentiation. It is important to note that corepressors typically interact with unliganded forms of the retinoid receptors and coactivators typically interact when the ligand is present (Weston, Hoffman et al. 2003).

1.4.4 Nuclear Orphan Receptors

Throughout the investigation of nuclear receptors and their functions, many receptors have been identified without any known ligands. As such, these receptors were referred to as nuclear orphan receptors (Giguere 1999). Due to the wide variety of nuclear orphan receptors, a classification system was developed where they were organized into seven groups according to the molecular phylogeny (Laudet 1997). Each group was then divided into families and each receptor within a family was identified with a Greek letter (Giguere 1999). Most nuclear orphan receptors are structurally similar to other nuclear receptors in that they have a highly recognizable LBD. The presence of the LBD is a strong indicator that all orphan receptors possess the ability to bind to a

specific ligand (Giguere 1999). To date, there are over 40 different nuclear orphan receptors. Studying them has resulted in the discovery of novel hormone response systems. Many nuclear orphan receptors and their ligands have been show to be associated with known diseases such as diabetes, atherosclerosis, and cancer. Thus, nuclear orphan receptors have opened new therapeutic avenues for the management of various diseases and demonstrated that they are excellent targets for drug development (Giguere 1999).

1.5 Retinoid-Related Orphan Receptors

The increasing body of knowledge about nuclear receptors and their involvement in many physiological processes has resulted in the identification of additional nuclear orphan receptors. The retinoid-related orphan receptor (ROR) subfamily is one class of nuclear orphan receptors that has been studied in depth. There are three different types of RORs, the retinoic acid receptor-related orphan receptor alpha (RORα), beta (-β) and gamma (-γ). The first ROR, RORα, was discovered in the early 1990s based on its sequence similarities with the retinoic acid receptor (RAR) and the retinoid X receptor (RXR) (Giguere, Tini et al. 1994). Each ROR gene generates several isoforms that differ only in their amino-terminus (Giguere, Tini et al. 1994; Hamilton, Frankel et al. 1996).

1.5.1 RORα Isoforms and Structure

RORα encodes four different isoforms known as RORα1-4, with all four being detected in humans but only isoforms α1 and α4 being detected in mouse (Jetten, Kurebayashi et al. 2001). Most of the isoforms exhibit a distinct pattern of tissue-specific expression and are involved in the regulation of a variety of physiological processes. The

two mouse specific isoforms of RORα encode proteins of 523 and 468 amino acids, respectively. RORα contains a typical nuclear receptor domain structure consisting of four major functional domains: an N-terminal domain followed by a highly conserved DNA-binding domain (DBD), a hinge domain, and a C-terminal ligand-binding domain (LBD) (Giguere 1999; Jetten, Kurebayashi et al. 2001). This nuclear orphan receptor regulates gene transcription by binding to specific retinoid-related orphan receptor DNA response elements (ROREs), consisting of the consensus RGGTCA motif preceded by an A/T rich sequence (Giguere, Tini et al. 1994; Giguere 1999; Jetten, Kurebayashi et al. 2001). RORα binds to its RORE as a monomer and does not form heterodimers (Giguere, Tini et al. 1994; Giguere 1999; Jetten, Kurebayashi et al. 2001). When bound to their RORE, all four isoforms of RORα constitutively recruit co-activators which results in transcription of their target genes (Atkins, Hu et al. 1999)

1.5.2 RORα Ligands

When the RORs were discovered, there were no known ligands for RORα. Recently, cholesterol, 7-dehydrocholesterol, and cholesterol sulfate were identified as RORα ligands (Kallen, Schlaeppi et al. 2002; Bitsch, Aichholz et al. 2003; Kallen, Schlaeppi et al. 2004). They were found to bind to RORα in a reversible manner and to enhance the RORE-dependent transcriptional activation by RORα. As such, it has been suggested that RORα may function as an important regulator of lipid metabolism.

1.5.3 Mouse Models of RORα Function

A variety of mouse models have been used to study the function of RORα. Interestingly however, RORα null mice exhibit an identical phenotype to that caused by a spontaneous mutation found in homozygous staggerer mice (Sg) (Hamilton, Frankel et al.

1996). This mutation produces a dominant negative RORα that results in a functional knockout phenotype. Specifically, the mutation is due to a 122bp deletion in the RORα gene resulting in the removal of the start of the ligand binding domain causing a frame shift and a premature stop codon (Hamilton, Frankel et al. 1996). Sg mice exhibit many abnormalities, many of them found in the brain. These mice show symptoms of ataxia and cerebellar dysfunction, which is characterized by fewer Purkinje cells and a loss of cerebellar granule cells (Hamilton, Frankel et al. 1996; Steinmayr, Andre et al. 1998). In addition, Sg mice have a susceptibility to atherosclerosis, hypo-α-lipoproteinemia, vascular dysfunction, muscular irregularities, osteoporosis, severe immune abnormalities and display abnormal blood lipid profiles with lower circulating plasma levels of high density lipoprotein C (HDL-C) and plasma triglycerides (Hamilton, Frankel et al. 1996; Steinmayr, Andre et al. 1998). Sg mice have also been found to have thinner long bones, reduced bone diameter, and are osteopenic compared to their wild type littermates (Meyer, Kneissel et al. 2000). In agreement with the characterized Sg mice phenotypes, it has been shown that RORα is expressed in a wide variety of tissues including the testis, kidneys, adipose tissue, liver, skeletal muscle, skin, thymus, lungs, and perhaps most abundantly in the cerebellum (Mamontova, Seguret-Mace et al. 1998; Jetten, Kurebayashi et al. 2001).

1.5.4 RORα and Lipid Metabolism

As a result of the staggerer phenotype displaying hypo-α-lipoproteinemia and lower levels of total plasma cholesterol, high density lipoprotein (HDL), and triglycerides (Hamilton, Frankel et al. 1996; Steinmayr, Andre et al. 1998), it was suggested that RORα plays an important role in lipid metabolism. In fact, RORα is now considered to

have an emerging and increasing role in regulating lipid metabolism in a multitude of tissues. The expression of fatty acid binding protein 3 (*Fabp3*), which is involved in lipid and fatty acid uptake, and of lipoprotein lipase (*Lpl*), which is involved in triglyceride hydrolysis, was reduced in C_2C_{12} skeletal muscle cells expressing a dominant-negative RORα (Lau, Nixon et al. 2004). Studies have also been performed by analyzing expression of putative down stream targets of RORα in the liver (Fitzsimmons, Lau et al. 2011). RORα controls the genetic programs involved in phase I and phase II metabolism, that regulate cholesterol homeostasis. For example, oxysterol 7α-hydroxylase (Cyp7b1) encodes an enzyme that regulates cholesterol homeostasis and has been identified as a RORα target gene (Kang, Angers et al. 2007). The isoform RORα1 has also been shown to interact directly with the mouse ApoA-1 gene promoter (Vu-Dac, Gervois et al. 1997). Recent investigations have proposed links between RORα and expression of the hepatic hormone FGF21 that has a number of ROREs within its promoter region (Wang, Solt et al. 2010). FGF21 has been recognized to being associated with stimulation of fatty acid oxidation in the liver (Wang, Solt et al. 2010). This suggests that RORα regulates expression of genes involved in lipid absorption, β-oxidation, cholesterol efflux, and energy expenditure in a variety of tissues. Furthermore, RORα has been identified as a promising therapeutic target in the treatment of obesity, type II diabetes, dyslipidemia, metabolic syndrome, and atherosclerosis (Lau, Nixon et al. 2004).

1.5.5 RORα in Endochondral Ossification

It has been found that RORα plays an important role in cartilage development. Staggerer mice display slower skeletal growth and delayed hypertrophic differentiation of chondrocytes (Tacchino et al, in prep). When three separate models of chondrocyte

hypertrophy were compared, RORα was one of the few genes that was upregulated in all models. Thus RORα has been suggested to be a marker of chondrocyte hypertrophy (Woods, James et al. 2009).

1.5.6 RORα Pharmacological Agents

Only one non-specific pharmacological agent has been used *in vitro* to investigate the physiological role of RORα (Kumar, Solt et al. 2010). The synthetic ligand, T0901317, was originally used as a liver X receptor (LXR) agonist however, recently it was found to act as an inverse agonist of RORα. T0901317 is the first potent inhibitor for RORα and RORγ (Kumar, Solt et al. 2010). The pharmacological effects of T0901317 have been characterized in detail with much of its activity attributed to LXRα and LXRβ activation (Michael, Schkeryantz et al. 2005). T0901317 was found to directly bind to RORα and RORγ resulting in a modification of the receptor's ability to interact with transcriptional co-activator proteins (Kumar, Solt et al. 2010). Unfortunately, it has been found that in addition to acting as a LXR agonist, T0901317 also activated the farnesoid X receptor (Houck, Borchert et al. 2004) and the pregnane X receptor (Mitro, Vargas et al. 2007). Due to the lack of specificity of this pharmacological agent there is great difficulty interpreting results obtained with this compound *in vitro* and *in vivo.*

1.6 Lipid Metabolism in Endochondral Ossification

In 1982, Kirkpatrick et al. (Kirkpatrick, Mohr et al. 1982) proved that chondrocytes contain lipid droplets. Since then very little research has been done to elucidate the relationship between chondrocytes, specifically chondrocyte differentiation, and lipid metabolism. Recently, it has been shown that there is a relationship between the nuclear

receptor PPARγ2 and chondrocyte lipid metabolism (Stanton, Li et al. 2010). This study showed that during differentiation, chondrocytes increase expression of *Lpl* and *Fabp4* (Stanton, Li et al. 2010). Lpl is involved in the hydrolysis of lipoprotein triglycerides into free fatty acids and is responsible for the uptake of free fatty acids while Fabp4 facilities uptake of long chain fatty acids and low density lipoproteins. This increase in *Lpl* and *Fabp4* is accompanied by an increase in *PPARγ2* gene expression. Moreover, cholesterol itself has been proven to promote endochondral bone growth and chondrocyte hypertrophy *in vitro* and to stimulate chondrocyte expression of genes linked to lipid metabolism, such as *Fabp4, Lpl,* and *Pdk4* (Woods, James et al. 2009). Since RORα is a receptor for cholesterol, it is possible that it plays a key role in the control of these genes in chondrocytes.

1.7 *In Vitro* Models Used to Study Chondrocytes

1.7.1 The ATDC5 Cell Line

The pre-chondrogenc cell line, ATDC5, has been established as an appropriate model to study chondrogenesis (Shukunami, Shigeno et al. 1996). Other cell lines such as RCJ3.1 and CFK2 have been used to study skeletal development but they are isolated from fetal calvariae, cells that undergo intramembranous ossification, and therefore are not an ideal model to study the endochondral pathway (Shukunami, Shigeno et al. 1996). Originally derived from AT805 mouse embryonal carcinoma (EC) cells, ATDC5 cells assume a fibroblastic shape when they are cultured to form a monolayer (Shukunami, Shigeno et al. 1996). The advantage of the ATDC5 cell line is that they can go through the entire pathway of chondrocyte differentiation. These cells proliferate at a high rate

until replication terminates as a result of contact inhibition. Insulin supplementation however, induces these cells to undergo chondrogenesis, chondrocyte differentiation, and matrix mineralization (Shukunami, Shigeno et al. 1996; Shukunami, Ishizeki et al. 1997). When ATDC5 cells undergo chondrogenesis, cells in the center of the monolayer continue to replicate forming cellular aggregates that are indicative of cartilaginous nodules. These cells produce an extracellular matrix rich in proteoglycans and type II collagen. At later stages, ATDC5 cells undergo hypertrophy, which is associated with an increase in type X collagen gene expression, an increase in alkaline phosphatase activity, and mineralization (Shukunami, Ishizeki et al. 1997).

1.7.2 Murine Micromass Culture System

Although the ATDC5 cell line is a convenient and frequently used model to study chondrogenesis and chondrocyte differentiation *in vitro*, there are other systems that are thought to more closely resemble the actual endochondral pathway. One such system is the use of limb bud mesoderm in what is known as the micromass culture system. Here, forelimbs and hindlimbs of embryonic day 11.5 (E11.5) mouse embryos are dissected and enzymatically digested. Mesenchymal cells are subsequently extracted and plated in a high density micromass culture which allows the mesenchymal cells to preferentially undergo chondrogenesis (Ahrens, Solursh et al. 1977). Specifically, mesenchymal cells within the micromass form aggregates, which then differentiate into chondrocytes. As they stabilize and proliferate, they produce an extracellular matrix. Overall, the process of chondrocyte differentiation in micromass culture closely follows the progression of limb mesenchyme maturation *in vivo* (Cash, Bock et al. 1997).

Previous studies have shown that cell density is a crucial factor to allow for chondrogenesis to occur in the micromass cultures (Ahrens, Solursh et al. 1977). At the optimal cell density of 2 x 10^5 cells per mass, pre-cartilagenous condensations are said to first appear after two days in culture with cartilage nodules forming after three days (Cash, Bock et al. 1997). Supplementing these cultures with ascorbic acid and beta glycerophosphate favours chondrocyte maturation and matrix mineralization, which is said to occur at approximately day 9 of culture (Weston, Rosen et al. 2000).

1.7.3 Tibia Organ Culture System

Previous studies in our lab have used a tibia organ culture system where tibiae are dissected from E15.5 mice and cultured for six days (Agoston, Khan et al. 2007). This *in vitro* approach is used primarily to determine bone growth in the absence of any endocrine regulation. The day of tibiae dissection is considered to be experimental day zero, as the tissues are allowed to recover from dissection overnight in distinct organ culture media. Bone length measurements are taken on days 1 and 6 with results expressed as a change in length relative to day 1. After the culture period is complete, tibiae can be fixed, sectioned, and analyzed for growth plate cell architecture, immunohistochemistry, immunofluorescence, and many other protocols (Agoston, Khan et al. 2007).

1.8 Hypothesis and Overall Objectives

The important role of retinoic acid receptor-related orphan receptor alpha is becoming increasingly evident in many biological tissues and physiological processes.

The relevance of this nuclear orphan receptor in chondrogenesis, chondrocyte differentiation, and endochondral bone growth however, has yet to be investigated. The studies described in this thesis will provide valuable insight into chondrocyte physiology during skeletal development and the pathogenesis of many skeletal diseases. They will ultimately contribute to improved understanding of complex molecular pathways that take place during bone development and hopefully lead to improved treatments of many skeletal malformations.

1.8.1 Hypothesis: RORα Promotes Expression of Lipid Metabolism Genes During Chondrocyte Differentiation

1.8.2 Objective One: Examine the role of RORα during chondrocyte differentiation and skeletal development *in vitro*

1.8.3 Objective Two: Examine the regulation of lipid metabolism genes and proteins by RORα *in vitro*

CHAPTER TWO

MATERIALS AND METHODS

2.1 Materials

Timed pregnant CD1 mice were purchased from Charles River Laboratories (St. Constant, Quebec, Canada). Unless otherwise stated, cell culture and organ culture media components were purchased from Sigma and Invitrogen. The RORα inverse agonist, T0901317, was purchased from Sigma. The expression vectors for mouse RORα, pCMV6 empty expression vector, and RORα mouse shRNA were purchased from Origene (Rockville, MD). Hoechst 3342 nuclear acid stain was purchased from MolecularProbes. Antibodies against Lipoprotein Lipase (catalogue number ab21356), RORα (catalogue number ab60134), and Myc tag (catalogue number ab9106) were purchased from Abcam (Cambridge, MA). The antibody against p57 (catalogue number sc-8298) was purchased from Sigma.

2.2 Methods

2.2.1 Murine Micromass Cultures

Micromass cultures were prepared as described (Ahrens, Solursh et al. 1977; Cash, Bock et al. 1997; Weston, Rosen et al. 2000; Stanton, Sabari et al. 2004) with minor modifications. Forelimbs and hindlimbs of up to 20 litters of E11.5 CD1 mouse embryos were dissected in Puck's Saline A buffer (PSA). The isolated limb buds were digested in 10 mg/ml dispase (Roche Molecular Biochemicals, Indianoapolis, IN) solution containing 10% fetal bovine serum (FBS)/PSA for 1.5-2 hours at 37°C and shaken at 120 rpm. Once the tissue was fully digested, the enzymatic reaction was neutralized with 2:3 Dulbecco's Modified Eagles Medium (DMEM): F12 media containing 10% FBS, 0.25% Pennicilin (10,000 units/ml)/Steptomycin (10,000 μg/ml),

and 0.25% L-glutamine (200mM). Digested tissue was ultimately passed through a 40μm cell strainer (Falcon, Lincoln Park, NJ) to explicitly extract cells. The cells were centrifuged for 5 minutes at 23°C at 1000 rpm, then resuspended in DMEM: F12 media containing 10% FBS, 0.25% Pennicilin/Steptomycin, and 0.25% glutamine. Cells were counted using a hemocytometer (Hausser Scientific Partnership, Horsham, PA, Catalogue number 3200), briefly centrifuged, resuspended at a final concentration of 2.5 $X10^7$ cell/ml and plated in eight 10 μl droplets into a six well NUNC delta surface cell culture plate (Nalge Nunc International, Rochester, NY, Catalogue number 140675). Cells were allowed to adhere to the plates by incubating for 1 hour at 37°C and 5% CO_2. Subsequently, 2ml of 2:3 DMEM:F12 media containing 10% FBS, 0.25% Pennicilin/Steptomycin, and 0.25% glutamine was added to the wells. Micromasses were cultured for a period of 12 days with media changed and supplemented with 50 μg/ml ascorbic acid (Sigma) and 1 mM beta-glycerol phosphate (Sigma) each day to differentiate the cells into chondrocytes (Stanton, Sabari et al. 2004). Media was also supplemented every 24 hours with dimethylsufoxide (DMSO) or 20 μM T0901317 (dissolved in DMSO).

2.2.2 ATDC5 Cell Culture and Generation of Stable Transfectants

The teratocarcinoma-derived cell line, ATDC5, was used to examine chondrogenesis *in vitro* (Shukunami, Shigeno et al. 1996). The ATDC5 cell line is prechondrogenic and chondrogenesis can be induced by supplementation with Insulin-transferrin-sodium selenite media (Shukunami, Shigeno et al. 1996). Cells were cultured in 47.5% DMEM, 47.5% F12, 5% FBS, 0.25% glutamine, and 0.25% Penicillin Steptomycin. Twenty-four hours post seeding, cells were treated with 1% Insulin-

transferrin-sodium selenite media (Sigma) as described (Wang, Woods et al. 2004). Media was changed every two days up to day fifteen of culture. For generation of stable transfectants, ATDC5 cells were cultured and transfected as described (Wang, Woods et al. 2004). Cells were plated at a density of 2 X 10^4 cells/ml per well in six-well tissue culture plates. Once the cells reached 50-80% confluency, they were individually transfected with expression vectors for mouse RORα (Origene, Rockville, MD), empty expression vector pCMV6 Entry (Origene, Rockville, MD), RORα Mouse shRNA (Origene, Rockville, MD), and HuSH shRNA RFP cloning vector (Origene, Rockville, MD). Pools of cells transfected with RORα expression vector or pCMV6 Entry were selected with 800 mg/ml Geneticin, and pools of cells transfected with RORα Mouse shRNA were selected with 5 ug/ml Puromycin. ATDC5 cells and stable transfectants were cultured for a period of 15 days with media changed every 48 hours.

2.2.3 Staining Methods

Micromass cultures were stained for chondrogenic differentiation with Alcian Blue (Sigma), which stains for glycosaminoglycan production. Cells were washed with phosphate-buffered saline (PBS), fixed for 1 hour in a 10% formalin solution and then washed again with PBS. Alcian Blue 8Gx was added to the cells and allowed to incubate overnight at room temperature. The following day excess stain was removed and the cells were rinsed with 70% ethanol and air-dried before visualization (Stanton, Sabari et al. 2004). Following visualization, Alcian Blue stained micromass cultures were incubated in 500 µl of 6M Guanidine hydrochloride overnight to exact the stain, as described (Shioi, McMullen et al. 2002). Absorbance of Alcian Blue staining was measured using a Safire Tecan Microplate Reader at 620 nm. Terminal chondrocyte

differentiation was visualized by staining for alkaline phosphatase (ALP) activity as described (Stanton, Sabari et al. 2004). Cells were washed with PBS, fixed for 1 hour in a 10% formalin solution, and washed again double distilled water for 15 minutes. A solution containing 0.1 mg/ml naphthol AS-MX phosphate (Sigma), 0.5% N,N-dimethylformamide, 2 mM $MgCl_2$, and 0.6 mg/ml Red Violet LB salt (Sigma) in 0.1 M Tris/HCl (pH 8.3) was added to the cells, and the micromass cultures were incubated in a dark environment for 45 minutes. After the incubation time, excess stain was removed and the cells were washed with double distilled water, then air-dried until visualization. To visualize calcium deposition and mineralization, Von Kossa staining was used. Cells were washed with PBS and fixed with 10% formalin solution. Micromasses were stained with ALP as above before staining with 2.5% silver nitrate solution for 30 minutes. Cells were then washed with water and allowed to air-dry before visualization (Stanton, Sabari et al. 2004). All images were taken using a Leica EC3 microscope and Leica Application Suite V3 software.

2.2.4 DNA Content Measurement of Micromass Cultures using Hoechst Staining

Quantification of DNA content in micromass cultures was performed using the UV-excitable DNA stain Hoechst 3342 at a concentration of 5 μg/ml. Micromass cultures plated in parallel to the previous discussed stains were cultured, treated, and fixed as previously mentioned. Cultures were then washed with PBS and incubated with Hoechst DNA dye for 15 minutes at 37°C. Following the incubation, cells were washed with PBS and incubated in a 1:1 trypsin:collagenase solution for 30 minutes. The cells were then centrifuged at 1000 rpm for 5 minutes and resuspended in culture media. Resuspended cells were used to measure DNA content using a fluorometer (Model RF-

M2004, Photon Technology International, London, ON) with excitation at 350 nm and emission at 450 nm. Data from 3 independent trials was analyzed using Felix32 software.

2.2.5 Protein Isolation and Western Blotting

Micromass cultures were washed with PBS and incubated in RadioImmuno Precipitation Assay (RIPA) lysis buffer for 30 minutes on ice. Cell lysates were then sonicated and collected after a 30 minute centrifugation at 4°C at 12, 000 x g. Protein was subsequently quantified by bicinchoninic acid (BCA) assay (Sigma) according to manufacturer's recommendations. To analyze protein levels, protein was diluted to 25 ng/μl, combined with double distilled water, NuPAGE Sample Reducing Agent (10x) (Invitrogen), NuPAGE LDS Sample Buffer (4x) (Invitrogen) and run on a NuPAGE 4-12% Bis-Tris Gel (Invitrogen). Protein was then transferred to an Immun-Blot PVDF Membrane (Bio-Rad, Hercules, CA, USA). Nonspecific protein sites were blocked using a 5% non fat milk powder in 1x TBST. The membrane was incubated overnight at 4°C in mouse monoclonal primary antibody to lipoprotein lipase IgG (Abcam), washed three times in 1x TBST for 8 minutes, and then incubated for one hour in horse radish peroxidase (HRP) conjugated-secondary antibody. An additional three eight minute washes in 1x TBST were performed. Signal was detected using ECL Plus Western Blotting Detection System (GE Healthcare, Baie d'Urfe, QB) and visualization was performed using a Konica Minolta SRX-101A developer.

2.2.6 RNA Isolation and Quantitative Real-Time Polymerase Chain Reaction

In the ATDC5 cell culture experiments, total RNA was isolated on days 3, 6, 9, 12, and 15 days using an RNeasy kit (Qiagen), according to manufacturer's instructions. In the micromass culture experiments, total RNA was isolated on days 3, 6, 9 and 12

using an RNeasy kit (Qiagen), according to manufacturer's instructions. RNA was quantified using a ND-1000 nanodrop. After concentrations were obtained, RNA was diluted to 40 ng/μl for use in Quantitative Real-Time Polymerase Chain Reaction (qPCR). A 14 μl mixture of specific target primers and probes generated from Applied Biosystems TaqMan Assays-on-Demand and a Taqman one-step mastermix kit (Applied Biosystems) was combined with 1 μl RNA for a final volume of 15 μl. The ABI Prism 7900 HT sequence detector (PerkinElmer Life Sciences) was used to detect amplified target sequences. All analyses were performed in triplicate for each time point, and data are a combination of a minimum of three independent trials. Real-Time expression values were calculated relative to the internal control glyceraldehyde-3-phosphate-dehydrogenase (*Gapdh*) using the relative quantification ΔΔCt analysis.

2.2.7 Organ Culture

Following euthanasia, E15.5 mouse tibiae were dissected and placed into twenty four well dishes containing sterile Organ Culture Media containing α-MEM, ascorbic acid, beta-glycerophosphate, bovine serum albumin, glutamine, and Penicillin/Streptomycin on ice as described (Agoston, Khan et al. 2007; Ulici, Hoenselaar et al. 2009). Tibiae were dissected using dissection forceps and a Zeiss Stereo Zoom Microscope Stemi SV6. Following dissections, tibiae were washed with sterile PBS. Fresh sterile organ culture media was then added to the plates and incubated at 37°C and 5% CO_2. The following day, bone length was measured using an eyepiece ruler on the Zeiss Stereo Zoom Microscope Stemi SV6, and an inverse agonist in varying concentrations was added to the culture (DMSO vehicle or 1 , 5, 10 or 20 μM T0901317 (Sigma)). Medium including treatments were changed every other day, and after 6 days

tibiae were measured again. Bone growth was determined by the difference in length between day 6 and day 1. One subset of tissues were then fixed in 4% paraformaldehyde overnight. These bones were labeled using 2% Mercurochrome (Alpha, catalogue number 1011965) and sent to the Molecular Pathology Core Facility, Robarts Research Institute, for tissue processing, paraffin embedding, and sectioning at a depth of 5 μm. Another subset of bones were incubated overnight in 70% ethanol followed by an overnight incubation in acetone. Bones were then incubated for two hours in Alcian Blue/Alizarian Red solution.

2.2.8 Histology and Immunohistochemistry

Paraffin embedded sections were dewaxed in Xylene for 8 minutes and 5 minutes, respectively, followed by rehydration in 2 x 100% ethanol, 95% ethanol, and 70 % ethanol for 2 minutes each. Histological Staining was performed using a Safranin O and Fast Green for 25 minutes and 7 minutes, respectively. Slides were then dehydrated and mounted using Xylene based mounting media. Immunohistochemistry was performed as previously discussed (Laron 2008) with minor modifications. Sections were incubated in 3% H_2O_2 for 15 minutes at room temperature to block endogenous peroxidases. Antigen retrieval was then performed by incubating sections in 10mM Sodium Citrate solution at pH6.0 at 95°C for 15 minutes. Sections were blocked with 5% goat serum and incubated with primary antibodies overnight at 4°C. The following day, sections were washed twice for 5 minutes in PBS and incubated for 1 hour in secondary antibody conjugated to HRP. Visualization was then performed using Liquid DAB+ Substrate Chromagen System (DAKO, catalogue number K3468). Slides were then counterstained with methyl

green solution. To analyze the images a Leica DM1000 microscope and Leica Application Suite V3 software were used.

2.2.9 Statistical Analysis

All data collected were from at least 3 independent trials. Data were expressed as mean ± SEM, and p values under 0.05 were considered significant (*). Statistical significance was determined with t-test or two way ANOVA followed by a post-hoc Bonferroni test using GraphPad Prism version 3.0 (GraphPad Software, San Diego, CA).

CHAPTER THREE

RESULTS

3.1 Treatment with T0901317 Results in Decreased Longitudinal Growth

In order to assess the influence of RORα inhibition on bone growth, I isolated tibiae from E15.5 mice. After extracting the tibiae, I cultured them for six days as described (Agoston, Khan et al. 2007; Ulici, Hoenselaar et al. 2009; Woods, James et al. 2009) with slight modifications. I measured the tibiae on day 1 and day 6. Bones were treated with either DMSO vehicle or the RORα inverse agonist T0901317 (in different concentrations) on day 1 and then every subsequent 48 hours. Data shows there is a significant decrease in bone growth between bones treated with DMSO vehicle and 20μM T0901317 (Figure 3.1A). Furthermore, a subset of the tibiae was stained with alcian blue/alizarin red to visualize cartilage (shown in blue) and the mineralized portion of the bone (shown in red). It can be seen that the overall length and the length of both the distal cartilage are reduced in the 20 μM T0901317 treated tibiae compared to the DMSO vehicle (Figure 3.1B). Together, this insinuates that RORα is crucial for proper skeletal growth.

3.2 Tibiae Treated with T0901317 Display Shortened Hypertrophic Zones

After I observed a decrease in bone growth with T0901317 treatment, I wanted to analyze how growth plate architecture was altered in this condition. Tibiae were cultured for a period of 6 days in T0901317 (20 μM) or DMSO vehicle and then sent for embedding in paraffin and sectioning (Robarts Research Institute, Molecular Pathology, London, Ontario, Canada). In order to assess growth plate organization, I performed

Figure 3.1 Treatment with T0901317 Results in Decreased Longitudinal Growth

E15.5 tibiae were grown and cultured for a period of 6 days and treated every 48 hours with medium containing DMSO vehicle, 1μM T0901317, 5μM T0901317, 10μM T0901317, or 20μM T0901317. Tibiae were measured on day 1 of culture and then at the end of day 6 for assessment of longitudinal growth. A) Tibiae treated with 20μM T0901317 had a significant reduction in growth compared to the control. Data shown are an average of 6 independent trials, ± SEM, * $p<0.05$. B) A subset of the tibiae was stained with alcian blue/alizarin red to visualize cartilage (shown in blue) and the mineralized portion of the bone (shown in red). Overall length and the length of the growth plates are reduced in the 20 μM T0901317 treated tibiae compared to the DMSO vehicle.

A

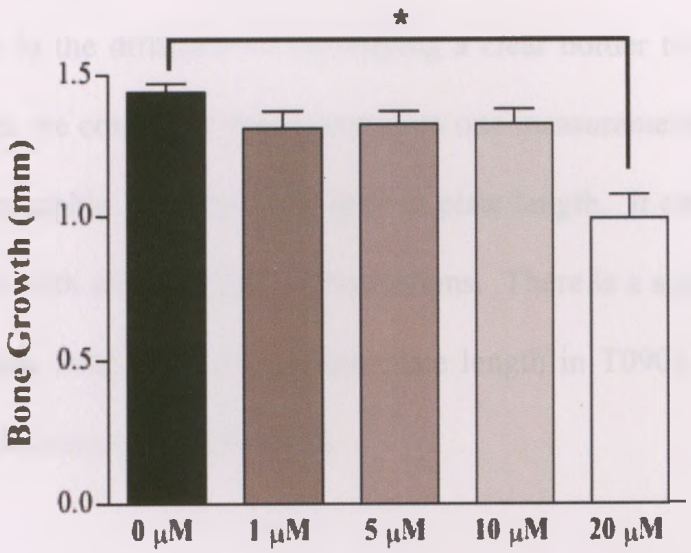

B

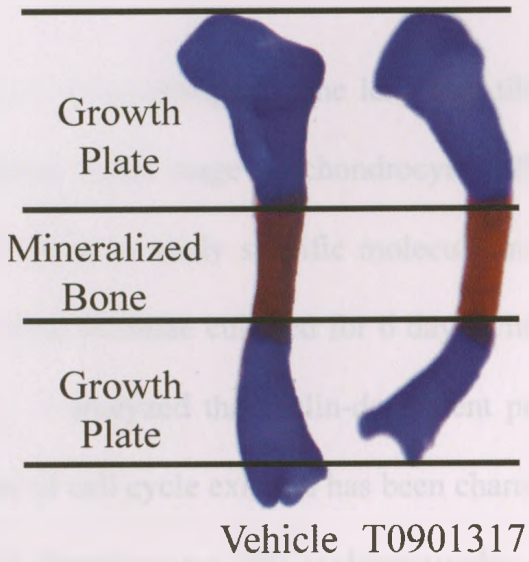

Vehicle T0901317

histological analyses using 0.1% Safranin O/0.02% fast green staining. The growth plate organization did not appear to be altered drastically with treatment; however, tibiae treated with T0901317 displayed shorter hypertrophic zones (Figure 3.2A). Furthermore, growth plate zone measurements were taken by a blinded observer in order to quantify my observations. Due to the difficulty of identifying a clear border between the resting and proliferative zones, we combined these zones into one measurement and compared to the length of the hypertrophic zone and total growth plate length. It can be seen that the quantitative data agree with my qualitative observations. There is a significant reduction in both the hypertrophic zone and total growth plate length in T0901317 treated tibiae compared to the vehicle control (Figure 3.2B).

3.3 p57 Protein Expression in Growth Plate is Decreased in RORα Inverse Agonist Treated Bones

Since I saw a reduction in hypertrophic zone length in tibia treated with 20 μM T0901317, I wanted to examine what stage of chondrocyte differentiation was being affected by the treatment. I chose to study specific molecular markers of chondrocyte differentiation and examine them in tibiae cultured for 6 days with T0901317 or DMSO using immunohistochemistry. I analyzed the cyclin-dependent protein kinase inhibitor, p57 (Kip2), which is a marker of cell cycle exit and has been characterized as a marker of the transition of proliferative chondrocytes into prehypertrophic chondrocytes (Zhang, Liegeois et al. 1997). In control bones I saw the expected staining for p57, with strongest expression at the transition from proliferating to prehypertrophic zones (Figure 3.3A).

Figure 3.2 Tibiae Treated with T0901317 Display Shortened Hypertrophic Zones

After 6 days in culture with DMSO vehicle or 20μM T0901317, tibiae were embedded in paraffin and sectioned. Growth plates were stained with safranin-o and fast green solution for visualization of growth plate organization and cell morphology. A) Growth plates treated with T0901317 displayed shortened hypertrophic zones (shown by arrows). Data shown are representative of 6 independent trials. B) Growth plate zones were measured from E15.5 tibiae treated with DMSO vehicle or 20 μM T0901317. Treatment with T0901317 resulted in a significant decrease in total growth plate length and hypertrophic zone length. n=6, $p<0.05$.

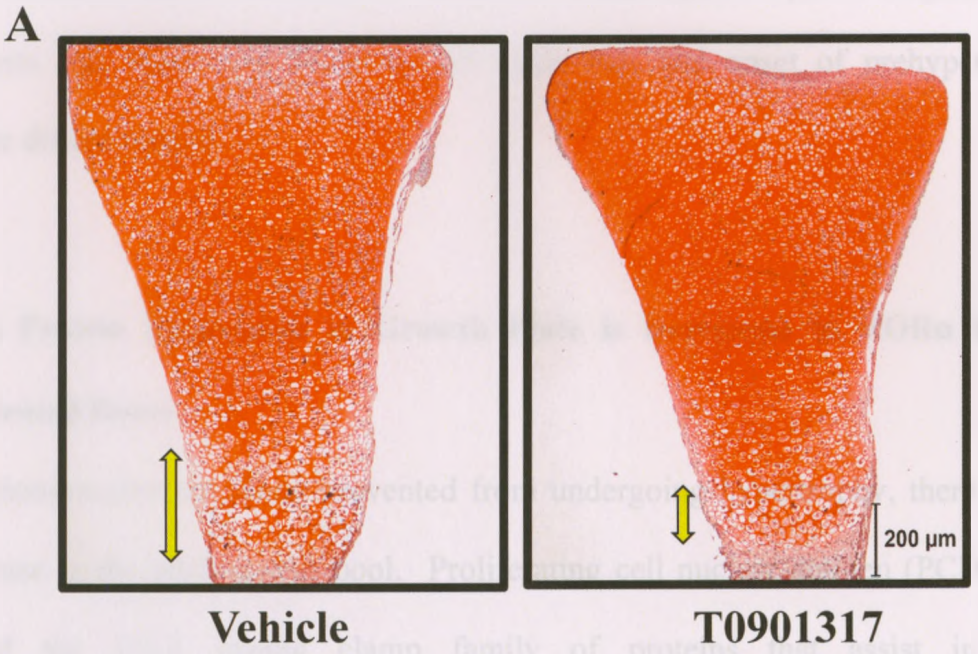
A
200 µm
Vehicle
T0901317

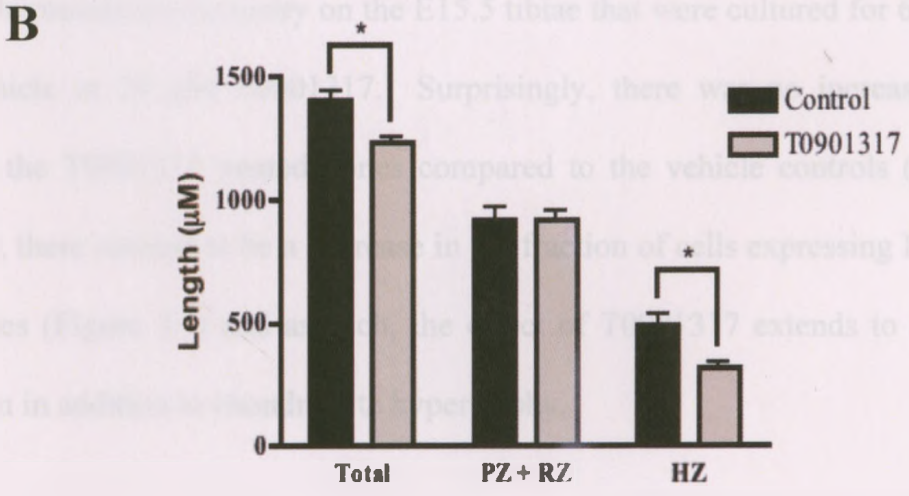
B
Length (µM)
1500
1000
500
0
Control
T0901317
Total
PZ + RZ
HZ

When treated with 20μM T0901317, p57 protein expression is decreased in the prehypertrophic zone (Figure 3.3A). I quantified the immunohistochemical staining using Leica Application Suite software and in agreement with the qualitative staining, there is a significant reduction in p57 staining in T0901317 treated growth plates (Figure 3.3B). This suggests that there is a delay in cell cycle exit and onset of prehypertrophic chondrocyte differentiation.

3.4 PCNA Protein Expression in Growth Plate is Decreased in RORα Inverse Agonist Treated Bones

If chondrocytes are being prevented from undergoing hypertrophy, there should be an increase in the proliferative pool. Proliferating cell nuclear antigen (PCNA) is a member of the DNA sliding clamp family of proteins that assist in DNA replication (Kelman and O'Donnell 1995) and is a marker of chondrocyte proliferation. I performed immunohistochemistry on the E15.5 tibiae that were cultured for 6 days with a DMSO vehicle or 20 μM T0901317. Surprisingly, there was no increase in PCNA staining in the T0901317 treated bones compared to the vehicle controls (Figure 3.4). Conversely, there seemed to be a decrease in the fraction of cells expressing PCNA in the treated bones (Figure 3.4) and as such, the effect of T0901317 extends to chondrocyte proliferation in addition to chondrocyte hypertrophy.

Figure 3.3 p57 Protein Expression in Growth Plates is Decreased in RORα Inverse Agonist Treated Bones

Tibiae were isolated from E15.5 mouse embryos, grown, and cultured for a period of 6 days. Tibiae were treated every 48 hours with medium containing DMSO vehicle or 20 μM T0901317. Tissues were fixed and prepared for histology.

A) Immunohistochemistry was performed with a p57 primary antibody followed by secondary antibody and visualization with the substrate DAB (dark brown staining). Extracellular matrix was counterstained with methyl green. Representative images show p57 protein levels highest in the prehypertrophic zone of control section; however, with treatment with RORα inverse agonist, p57 protein expression is decreased in this region. n=6. B) Immunohistochemical staining was quantified using Leica Application Suite software. There is a significant reduction in p57 staining in the T0901317 treated growth plates. n=5.

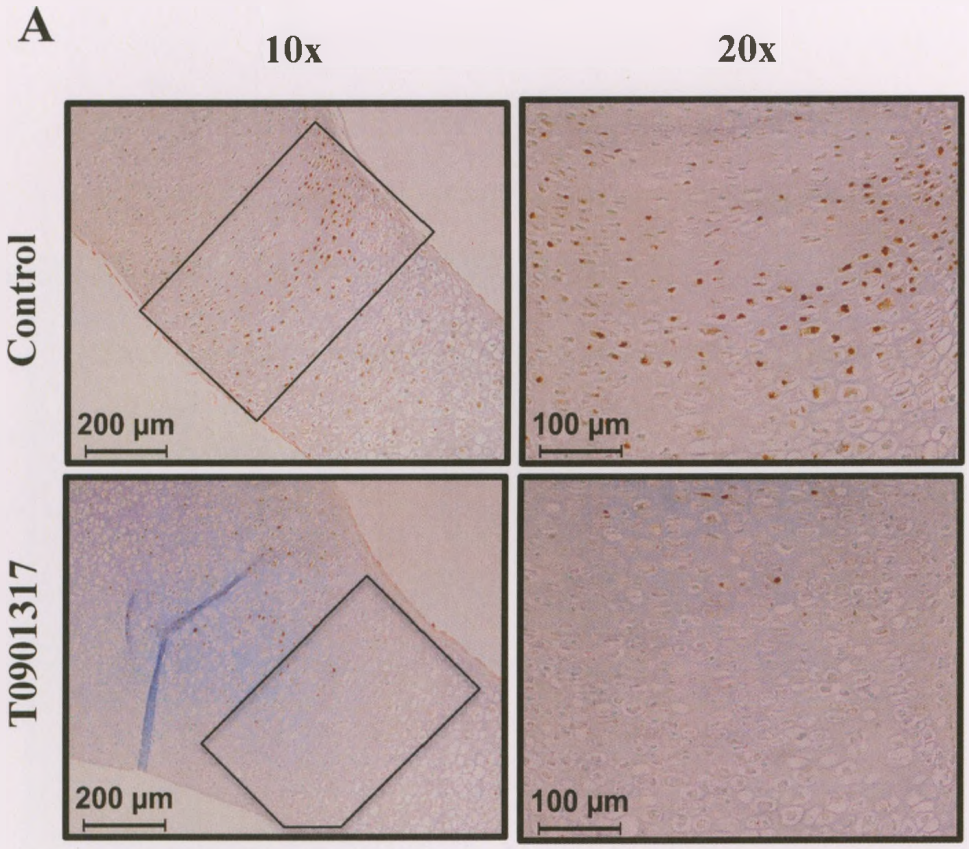
A
10x
20x
Control
T0901317
200 µm
100 µm
200 µm
100 µm

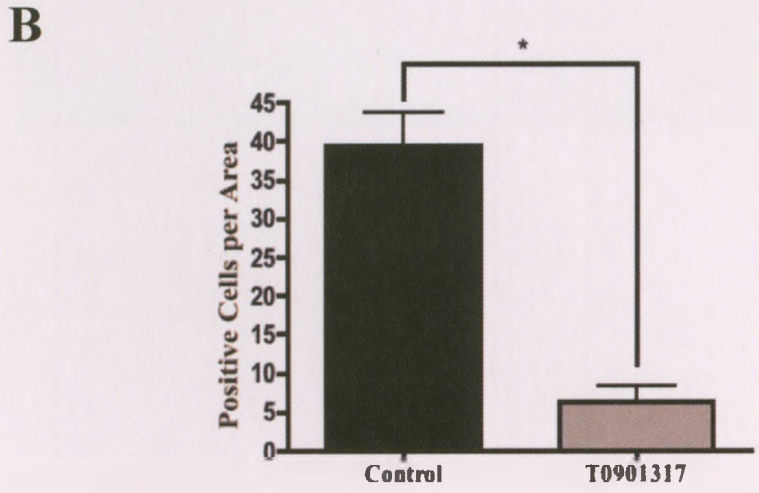
B
*
Positive Cells per Area
45
40
35
30
25
20
15
10
5
0
Control
T0901317

Figure 3.4 PCNA Protein Expression in Growth Plate is Decreased in RORα Inverse Agonist Treated Bones

Immunohistochemistry was performed on the E15.5 tibiae that were cultured for 6 days with a DMSO vehicle or 20 μM T0901317. Tissues were fixed and prepared for histology. There was a decrease in protein expression (dark brown staining) in the T0901317 treat bones compared to the DMSO controls. n=3.

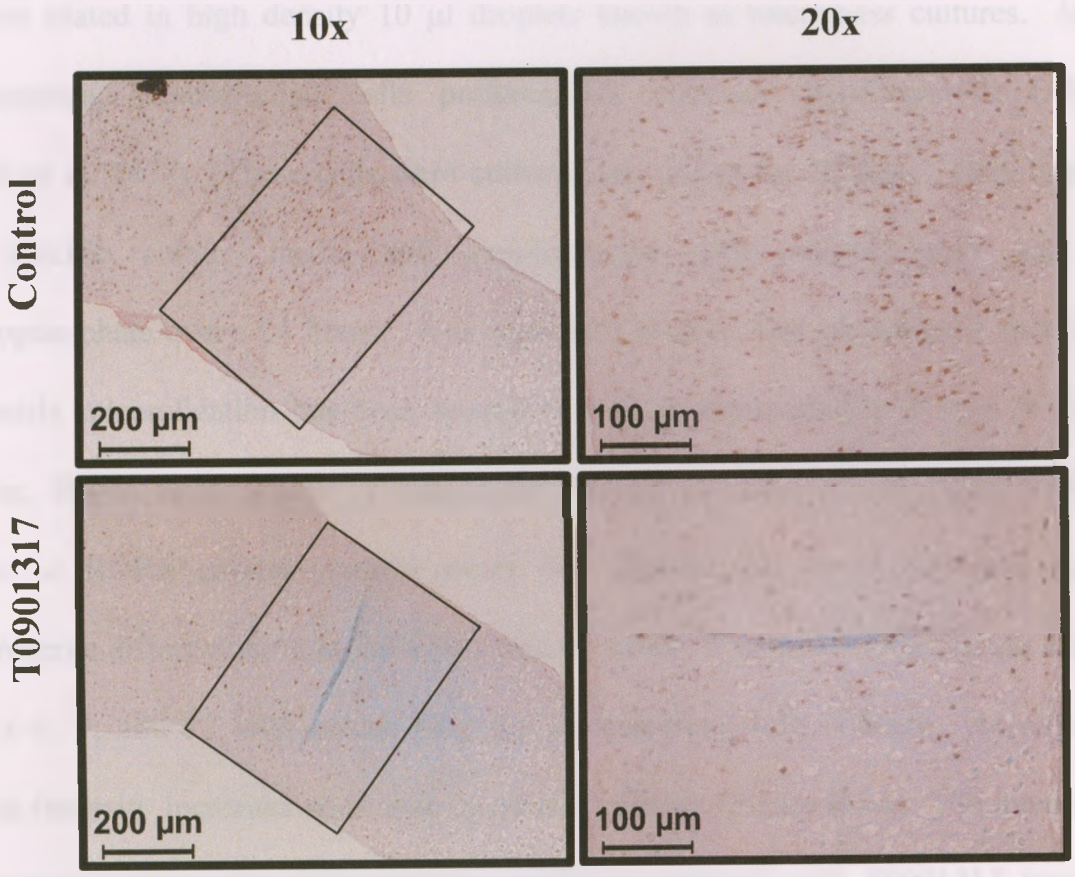
10x
20x
Control
T0901317
200 µm
100 µm
200 µm
100 µm

3.5 RORα Inhibition Results in Decreased Glycosaminoglycan Production

I next wanted to study the role of RORα during chondrocyte differentiation *in vitro*. One model that has been widely applied to study these processes is the use of limb bud mesoderm micromass cultures. In this system, forelimbs and hindlimbs of E11.5 mouse embryos are dissected and enzymatically digested. Once isolated, mesenchymal cells are plated in high density 10 µl droplets known as micromass cultures. In this configuration, mesenchymal cells preferentially undergo chondrogenesis (Ahrens, Solursh et al. 1977). These cells were cultured and grown for 12 days. They were fed with specific culture media and supplemented with ascorbic acid and beta glycerophosphate every 24 hours. It is important to note, that chondrocyte maturation and matrix mineralization has been proven to start at approximately 9 days of culture (Weston, Rosen et al. 2000). I treated the micromass cultures with either a DMSO vehicle or RORα inverse agonist every day starting on day 3 to allow natural chondrogenic differentiation in the initial culture period. I stained the micromass cultures at days 6, 9, and 12 with alcian blue for glycosaminoglycan content. As expected, staining intensity increased over time in control cultures (Figure 3.5A). The intensity of this staining and of this differentiation marker is reduced with T0901317 treatment (Figure 3.5A). I then quantified the alcian blue content of the micromasses by using a spectrophotometer at 620 nm after extraction with 6M Guanidine hydrochloride. Treatment with T0901317 resulted in significant decrease in absorbance levels (Figure 3.5B), thus correlating with the qualitative observations previously made and showing that inhibition of RORα function results in a decrease in markers of early chondrocyte differentiation.

Figure 3.5 RORα Inhibition Results in Decreased Glycosaminoglycan Production in Micromass Culture

Mouse embryonic mesenchymal limb bud cells were plated in micromass cultures and grown for 12 days with either DMSO vehicle or RORα inverse agonist (T0901317), starting on day 3. They were stained after 6, 9, and 12 days with Alcian blue for glycosaminoglycan content. A) The intensity of this staining and of this differentiation marker is reduced with T0901317 treatment. B) After 6, 9, and 12 days the Alcian blue content of the micromasses was quantified after extraction with 6 M Guanidine hydrochloride using spectrophotometry at 620 nm. Treatment with T0901317 resulted in decreased absorbance levels. $n=6$, $p<0.05$.

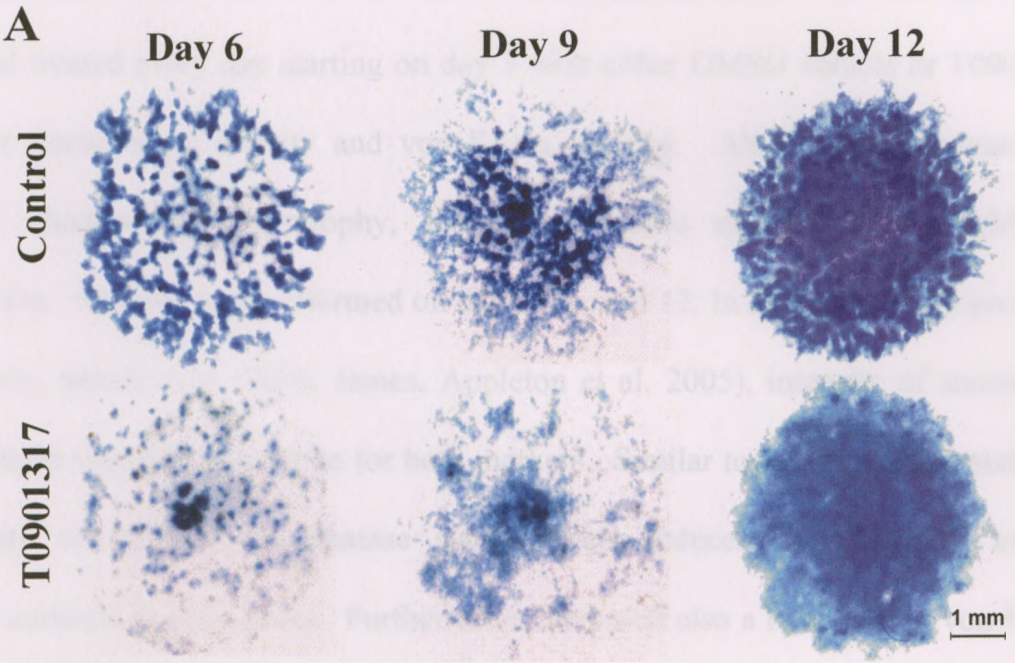
A
Day 6
Day 9
Day 12
Control
T0901317
1 mm

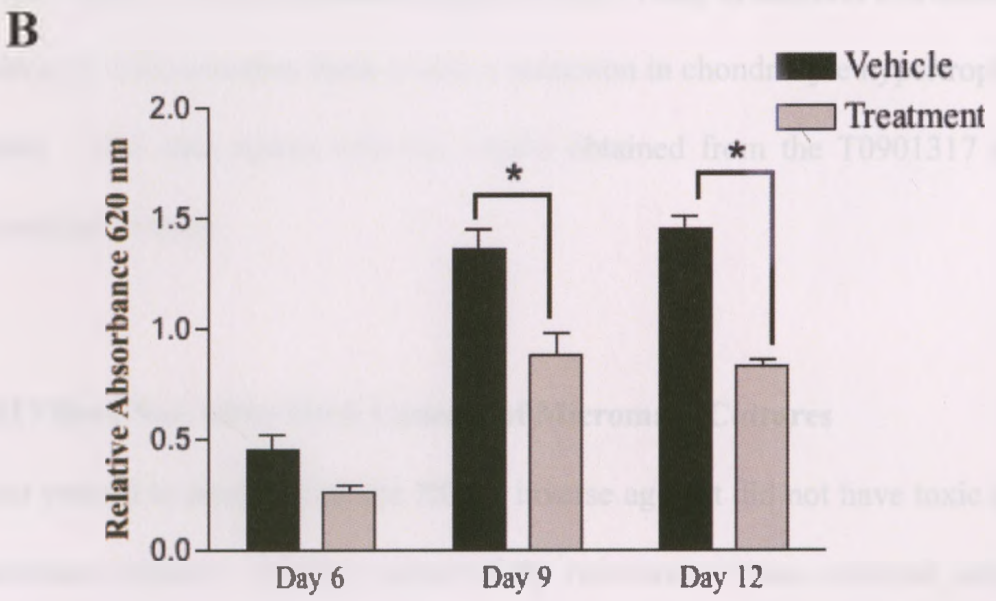
B
Vehicle
Treatment
Relative Absorbance 620 nm
2.0
1.5
1.0
0.5
0.0
*
*
Day 6
Day 9
Day 12

3.6 Treatment with RORα Inverse Agonist Results in Reduced Chondrocyte Hypertrophy and Mineralization

Next, I wanted to examine if there was also an effect on later stages of chondrocyte differentiation. I stained a subset of micromass cultures that were grown for 12 days and treated every day starting on day 3 with either DMSO vehicle or T0901317 for alkaline phosphatase activity and von Kossa staining. Alkaline phosphatase is a marker of chondrocyte hypertrophy, while von Kossa staining is a marker of mineralization. Staining was performed on days 6, 9, and 12. In agreement with previous data (Stanton, Sabari et al. 2004; James, Appleton et al. 2005), intensity of staining in control cultures increased over time for both markers. Similar to the alcian blue staining, the intensity of alkaline phosphatase staining was reduced in T0901317 treated micromass cultures (Figure 3.6A). Furthermore, there was also a reduction in von Kossa staining in the T0901317 treated cultures (Figure 3.6B). Thus, in addition to a decrease in early chondrocyte differentiation there is also a reduction in chondrocyte hypertrophy and mineralization. This data agrees with the results obtained from the T0901317 treated tibiae discussed previously.

3.7 T0901317 Does Not Affect DNA Content of Micromass Cultures

I next wanted to confirm that the RORα inverse agonist did not have toxic effects on the micromass cultures. Another subset of the micromasses was cultured, using the same protocol as previously described, so I could analyze the DNA content of the cultures. I performed this analysis on days 6, 9, and 12 days. To measure DNA content I used a Hoechst 33342 fluorescence stain. Measurements showed that

Figure 3.6 Treatment with RORα Inverse Agonist Results in Reduced Alkaline Phosphatase Activity and Mineralization

Mouse embryonic mesenchymal limb bud cells were plated in micromass cultures and grown for 12 days and treated with either DMSO vehicle or RORα inverse agonist (T0901317) on day 3. They were stained after 6, 9, and 12 days for various chondrocyte differentiation markers: A) Alkaline phosphatase activity and B) Von Kossa for mineralization. The intensity of both these markers are reduced in the T0901317 treated micromass cultures. n=6.

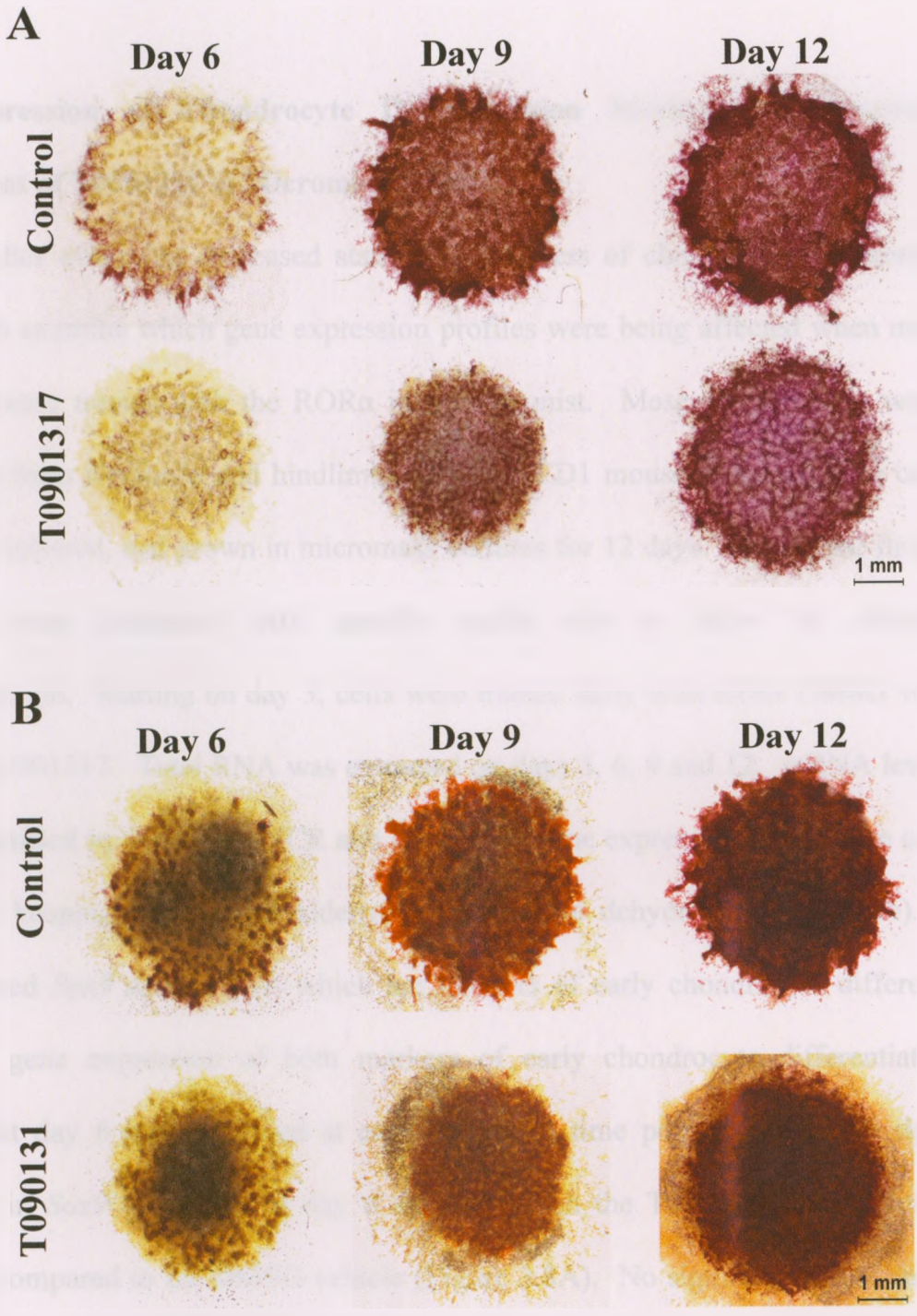
A
Day 6
Day 9
Day 12
Control
T0901317
1 mm
B
Day 6
Day 9
Day 12
Control
T090131
1 mm

treating the micromass cultures with T0901317 resulted in no significant changes in DNA content (Figure 3.7).

3.8 Expression of Chondrocyte Differentiation Markers is Decreased with Treatment of T0901317 in Micromass Cultures

After observing decreased staining in markers of chondrocyte differentiation, I wanted to examine which gene expression profiles were being affected when micromass cultures were treated with the RORα inverse agonist. Mesenchymal cells were again dissected from forelimbs and hindlimbs of E11.5 CD1 mouse embryos. The cells were isolated, cultured, and grown in micromass cultures for 12 days. During the first 3 days, cultures were incubated with specific media only to allow for chondrogenic differentiation. Starting on day 3, cells were treated daily with either DMSO vehicle or 20 μM T0901317. Total RNA was extracted on days 3, 6, 9 and 12. mRNA levels were then quantified by Real Time PCR and all relative gene expression levels were compared to house keeping gene, Glyceraldehyde 3 phosphate dehydrogenase (*Gapdh*). I first investigated *Sox9 and Col2a1*, which are markers of early chondrocyte differentiation. Relative gene expression of both markers of early chondrocyte differentiation was greatest at day 6 and decreased at each additional time point. There is a significant decrease in *Sox9* expression at day 6 and day 12 in the T0901317 treated micromass cultures compared to the DMSO vehicle (Figure 3.8A). No significance was detected at day 9 however, the same trend is evident on this day as the other time points (Figure 3.8A). Furthermore, although no statistical significance was found in *Col2a1* expression between the T0901317 treated and DMSO vehicle micromass cultures,

Figure 3.7 T0901317 Does Not Affect DNA Content of Micromass Cultures

Mouse embryonic mesenchymal limb bud cells were plated in micromass cultures and grown for 12 days and treated with either DMSO vehicle or RORα inverse agonist (T0901317) on day 3. To measure DNA content, Hoechst 33342 fluorescence stain was used. This was performed on days 3, 6, 9, and 12. Measurements showed that treating the micromass cultures with T0901317 did not result in significant changes in DNA content. n=3.

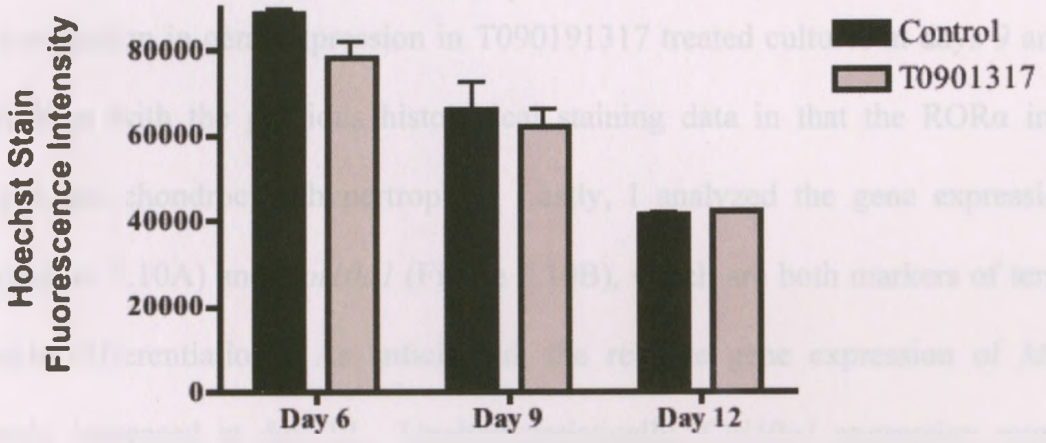
Hoechst Stain
Fluorescence Intensity
80000
60000
40000
20000
0
Day 6
Day 9
Day 12
Control
T0901317

there is also a decreasing trend at each time point in the treated cells (Figure 3.8B). Thus, both *Sox9* and *Col2a1* expression suggest that there is a decrease in early chondrocyte differentiation with treatment of the RORα inverse agonist.

To elucidate the role of T0901317 treatment on chondrocyte hypertrophy, I analyzed the relative gene expression of *Runx2* (Figure 3.9A) and alkaline phosphatase (Figure 3.9B). The gene expression profiles of both *Runx2* and alkaline phosphatase show that starting at day 9 there was a dramatic increase, which is when chondrocyte hypertrophy begins in micromass cultures (Weston, Rosen et al. 2000). Coincidently, there is a reduction in gene expression in T090191317 treated cultures at days 9 and 12. This correlates with the previous histological staining data in that the RORα inverse agonist reduces chondrocyte hypertrophy. Lastly, I analyzed the gene expression of *Mmp13* (Figure 3.10A) and *Col10a1* (Figure 3.10B), which are both markers of terminal chondrocyte differentiation. As anticipated, the relative gene expression of *Mmp13* significantly increased at day 12. Uncharacteristically, *Col10a1* expression remained relatively constant from day 6 to day 12. There was a statistically significant reduction in *Mmp13* gene expression at day 6 and day 12 upon treatment (Figure 3.10A). In addition, at every time point, there is a decreasing trend of *Col10a1* gene expression in the T0901317 treated micromass cultures compared to the DMSO vehicle (Figure 3.10B). Combined, these results signify that the RORα inverse agonist reduces expression of both early and late markers of chondrocyte differentiation.

Figure 3.8 Early Chondrogenic Gene Expression is Decreased with Treatment of T0901317 in Micromass Cultures

Mesenchymal cells dissected from forelimbs and hindlimbs of E11.5 CD1 embryos were plated and grown for 12 days in micromass cultures. Total RNA was extracted on days 3, 6, 9, and 12. Cultures were treated with either DMSO vehicle or 20 μM T0901317, starting on day 3. RNA was quantified by Real Time PCR. All relative gene expression levels were compared to house keeping gene *Gapdh* transcript levels. Relative transcript levels of various marker genes of early chondrocyte differentiation such as A) *Sox9* and B) *Col2a1* in control cultures decrease with micromass differentiation. Furthermore, there is a decrease in *Sox9* expression at days 6 and 12 with T0901317 treatment. There is a decreasing trend in *Col2a1* expression with T0901317 treatment. $n=6$, $p<0.05$.

A

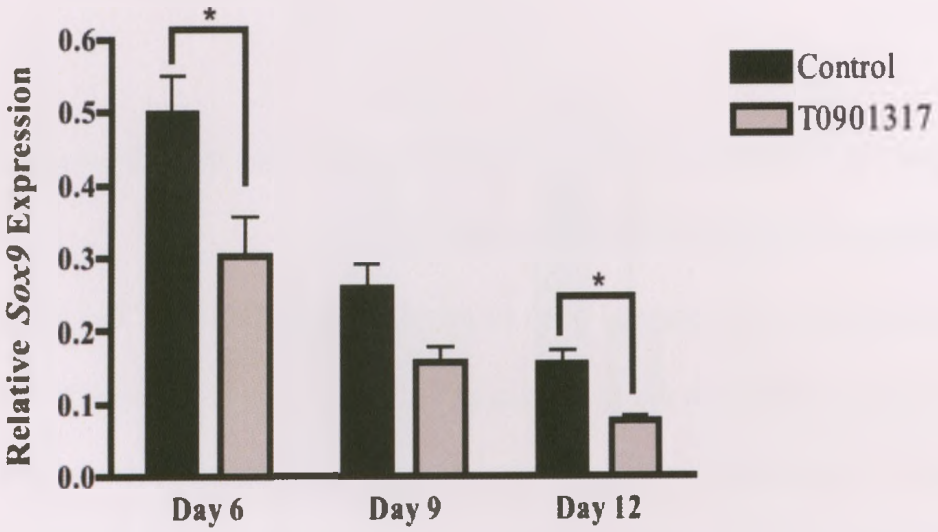
Relative Sox9 Expression
0.6
0.5
0.4
0.3
0.2
0.1
0.0
*
*
Day 6
Day 9
Day 12
Control
T0901317

B

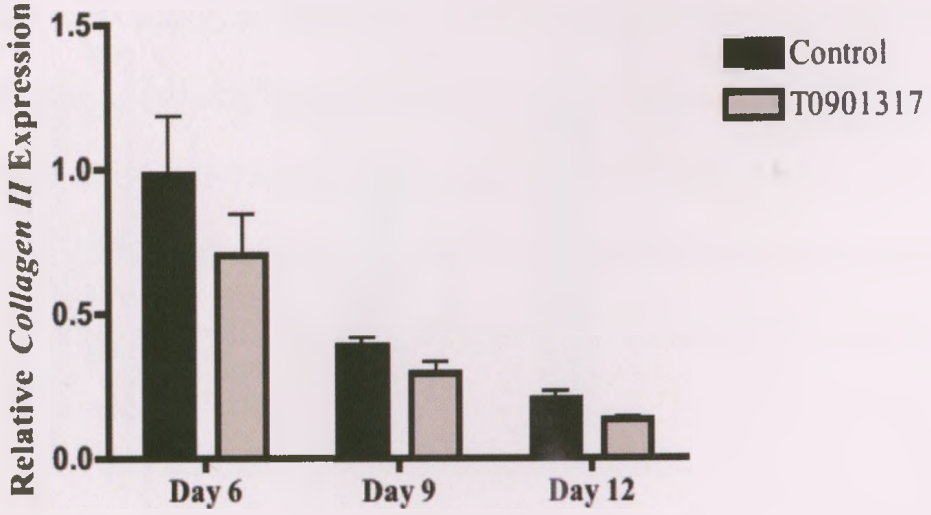
Relative Collagen II Expression
1.5
1.0
0.5
0.0
Day 6
Day 9
Day 12
Control
T0901317

Figure 3.9 Chondrocyte Hypertrophic Gene Expression is Decreased with Treatment of T0901317 in Micromass Cultures

Mesenchymal cells dissected from forelimbs and hindlimbs of E11.5 CD1 embryos were plated and grown for 12 days in micromass cultures. Total RNA was extracted on days 3, 6, 9, and 12. Cultures were treated with either DMSO vehicle or 20 μM T0901317, starting on day 3. RNA was quantified by Real Time PCR. All relative gene expression levels were compared to house keeping gene *Gapdh* transcript levels. Relative gene expression of markers of chondrocyte hypertrophy such as A) *Runx2* and B) Alkaline Phosphatase are dramatically increased at day 9 in control cultures. Additionally, treatment with T0901317 results in a significant decrease in both *Runx2* and Alkaline Phosphatase expression at days 9 and 12. $n=6$, $p<0.05$.

A

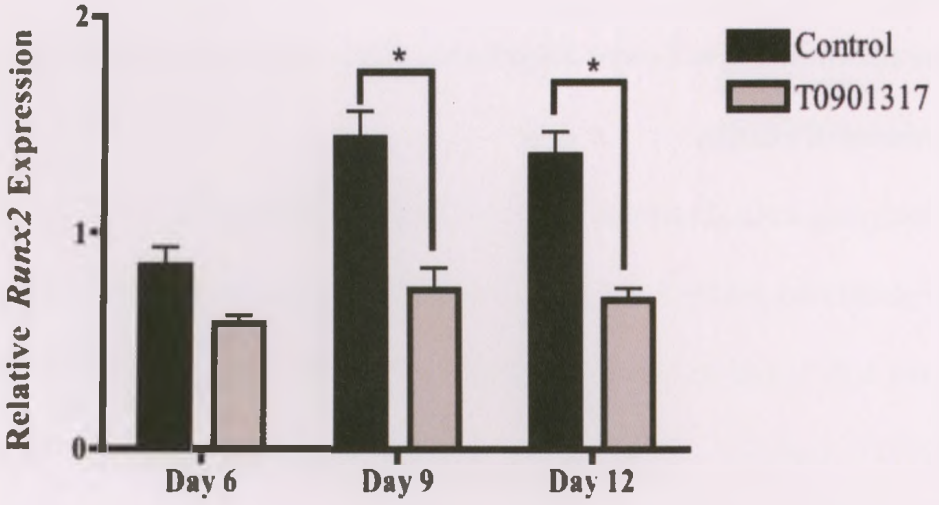
Relative Runx2 Expression
2
1
0
*
*
Day 6
Day 9
Day 12
Control
T0901317

B

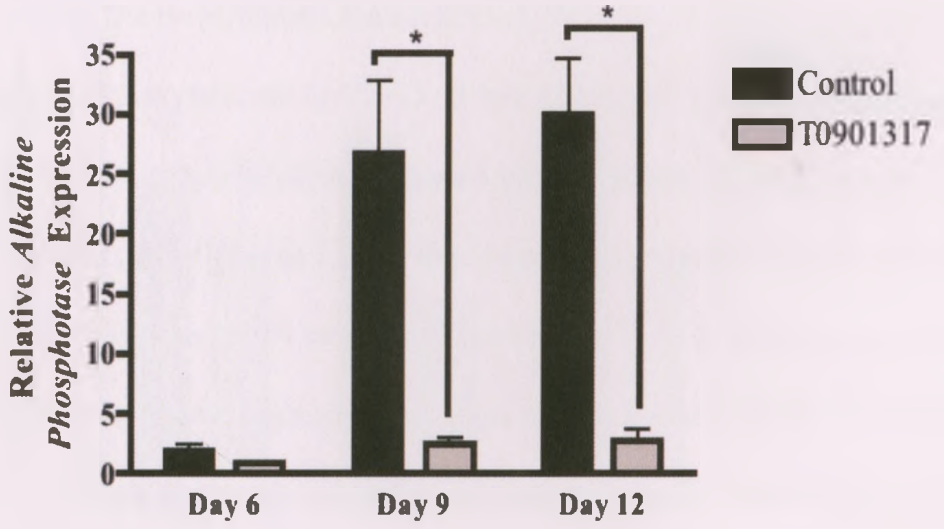
Relative Alkaline Phosphotase Expression
35
30
25
20
15
10
5
0
*
*
Day 6
Day 9
Day 12
Control
T0901317

Figure 3.10 Markers of Terminal Chondrocyte Differentiation and Mineralization Show Lower Expression upon Treatment of T0901317 in Micromass Cultures

Mesenchymal cells dissected from forelimbs and hindlimbs of E11.5 CD1 embryos were plated and grown for 12 days in micromass cultures. Total RNA was extracted on days 3, 6, 9, and 12. Cultures were treated with either DMSO vehicle or 20 μM T0901317, starting on day 3. RNA was quantified by Real Time PCR. All relative gene expression levels were compared to house keeping gene *Gapdh* transcript levels. Relative gene expression of markers of terminal chondrocyte differentiation and mineralization such as A) *Mmp13* and B) *Col10a1* are analyzed. A) Relative gene expression of *Mmp13* increases with chondrocyte differentiation and there is a reduction in gene expression at days 6 and day 12 of T0901317, relative to DMSO. B) Gene expression of *Col10a1* in control cultures remained relatively constant with chondrocyte differentiation and no significant decrease was detected between control and treated cultures. There is a decreasing trend at days 6, 9, and 12 in the T0901317 treated cultures. $n=6$, $p<0.05$.

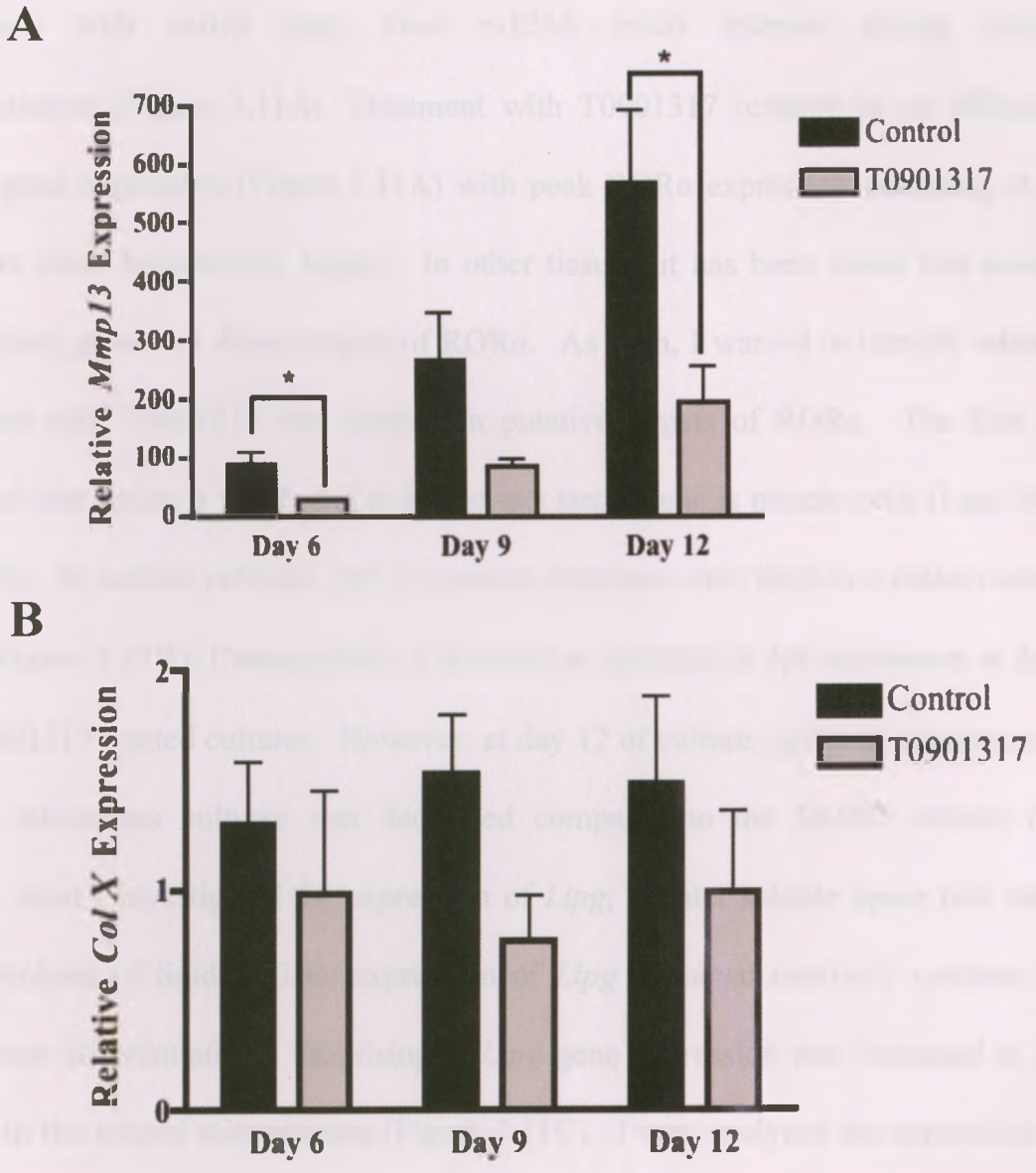
A
Relative Mmp13 Expression
700
600
500
400
300
200
100
0
*
*
Day 6
Day 9
Day 12
Control
T0901317
B
Relative Col X Expression
2
1
0
Day 6
Day 9
Day 12
Control
T0901317

3.9 Relative Gene Expression of Lipid Metabolism Genes is Altered with T0901317 Treatment

Next, I was interested in determining if the receptor itself was self-regulated. As such, I analyzed RORα gene expression in the micromass cultures as described above. In agreement with earlier data, *Rorα* mRNA levels increase during micromass differentiation (Figure 3.11A). Treatment with T0901317 resulted in no difference of RORα gene expression (Figure 3.11A) with peak RORα expression occurring at day 9, which is when hypertrophy begins. In other tissues, it has been found that some lipid metabolism genes are direct targets of RORα. As such, I wanted to identify what effect treatment with T0901317 was having on putative targets of RORα. The first gene I analyzed was *Lpl* as it was found to be a direct target gene is muscle cells (Lau, Nixon et al. 2004). In control cultures, *Lpl* expression increased over time in a pattern similar to *Rorα* (Figure 3.11B). Unexpectedly, I detected an increase in *Lpl* expression at day 6 in the T0901317 treated cultures. However, at day 12 of culture, *Lpl* gene expression in the treated micromass cultures was decreased compared to the DMSO vehicle (Figure 3.11B). Next I investigated the expression of *Lipg*, a water soluble lipase that catalyzes the hydrolysis of lipids. Gene expression of *Lipg* remained relatively constant during micromass differentiation. Surprisingly, *Lipg* gene expression was increased at days 9 and 12 in the treated micromasses (Figure 3.11C). I next analyzed the expression of the fatty acid carrier protein, fatty acid binding protein 3 (*Fabp3*). No significant differences were detected in *Fabp3* gene expression at any time points (Figure 3.12A). Another gene involved in lipid metabolism is pyruvate dehydrogenase kinase

Figure 3.11 Relative Gene Expression of Lipid Metabolism Genes is Altered with T0901317 Treatment

Mesenchymal cells dissected from forelimbs and hindlimbs of E11.5 CD1 embryos were plated and grown for 12 days in micromass cultures. Total RNA was extracted on days 3, 6, 9, and 12. Cultures were treated with either DMSO vehicle or 20 μM T0901317, starting on day 3. RNA was quantified by Real Time PCR. All relative gene expression levels were compared to house keeping gene *Gapdh* transcript levels. A) Relative gene expression data shows that in micromass cultures treated with T0901317, there is no significant difference in *RORα* transcript levels compared to control cultures. Peak expression of *RORα* occurs at day 9 of culture. B) In control cultures, *Lpl* gene expression is greatest at day 12. There is a statistically significant increase in *Lpl* expression at day 6 with a significant decrease at day 12 in T0901317 treated cultures. C) *Lipg* relative gene expression is increased at day 9 and maintained at day 12 in control cultures. There is a significant increase in T0901317 treated micromass cultures at days 9 and 12. $n=6$, $p<0.05$.

A

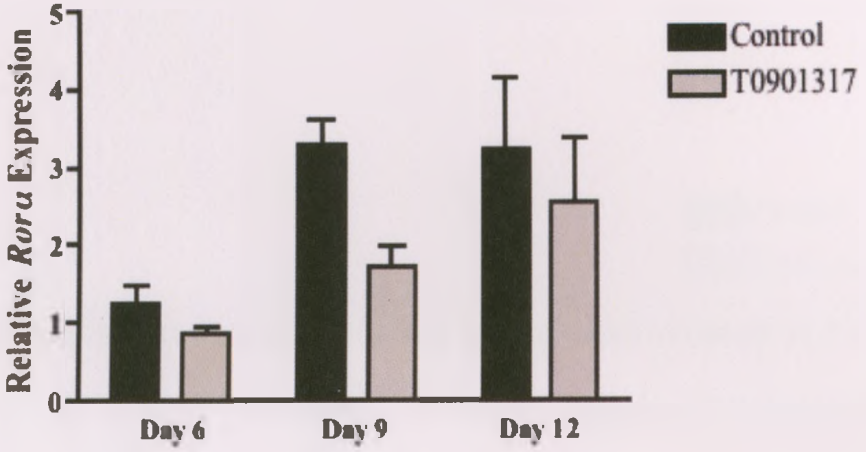
Relative Rora Expression
0
1
2
3
4
5
Day 6
Day 9
Day 12
Control
T0901317

B

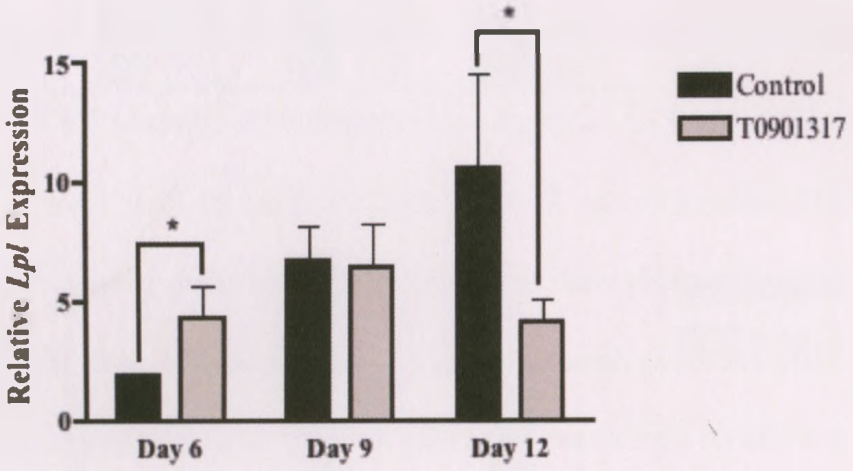
Relative Lpl Expression
0
5
10
15
*
*
Day 6
Day 9
Day 12
Control
T0901317

C

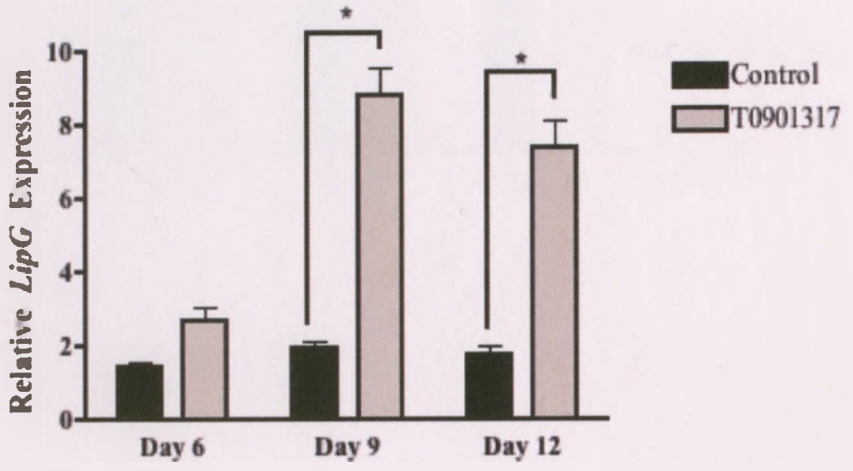
Relative LipG Expression
0
2
4
6
8
10
*
*
Day 6
Day 9
Day 12
Control
T0901317

Figure 3.12 Relative Gene Expression of *Fabp3* and *Pdk4* Genes is Unchanged with T0901317 Treatment

Mesenchymal cells dissected from forelimbs and hindlimbs of E11.5 CD1 embryos were plated and grown for 12 days in micromass cultures. Total RNA was extracted on days 3, 6, 9, and 12. Cultures were treated with either DMSO vehicle or 20 μM T0901317, starting on day 3. RNA was quantified by Real Time PCR. All relative gene expression levels were compared to house keeping gene *Gapdh* transcript levels. A) No difference was detected in *Fabp3* gene expression with T0901317 treatment. B) There was no significant difference in *Pdk4* gene expression in treated cultures however, there is a trend that suggests there is decreased *Pdk4* expression with treatment. $n=6$, $p<0.05$.

A

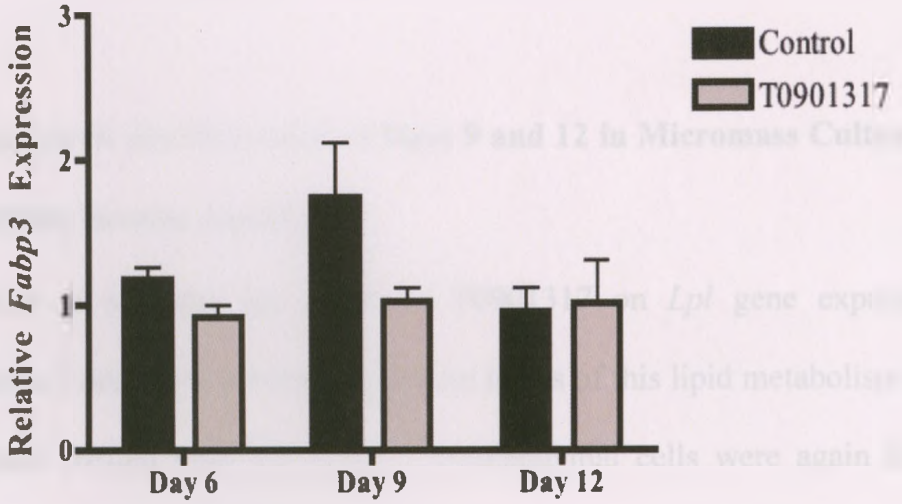
Relative Fabp3 Expression
3
2
1
0
Day 6
Day 9
Day 12
Control
T0901317

B

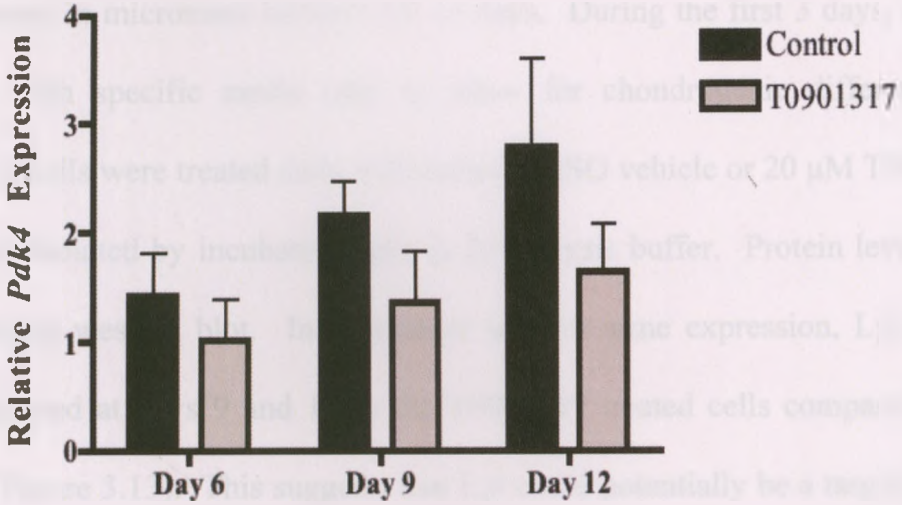
Relative Pdk4 Expression
4
3
2
1
0
Day 6
Day 9
Day 12
Control
T0901317

isozyme 4 (*Pdk4*). In the control cultures, *Pdk4* expression increased with micromass differentiation. There was no statistically significant difference detected between the T0901317 treated micromass cultures and DMSO controls, however, there is a decreasing trend at every time point with treatment (Figure 3.12B).

3.10 Lpl Protein Levels are Decreased at Days 9 and 12 in Micromass Cultures with Treatment of RORα Inverse Agonist

In addition to studying the effect of T0901317 on *Lpl* gene expression in micromass cultures, I desired to investigate protein levels of this lipid metabolism gene in micromass cultures treated with T0901317. Mesenchymal cells were again dissected from forelimbs and hindlimbs of E11.5 CD1 mouse embryos. The cells were isolated, cultured, and grown in micromass cultures for 12 days. During the first 3 days, cultures were incubated with specific media only to allow for chondrogenic differentiation. Starting on day 3, cells were treated daily with either DMSO vehicle or 20 μM T0901317. Total protein was isolated by incubating cells in RIPA lysis buffer. Protein levels were then analyzed using western blot. In agreement with its gene expression, Lpl protein levels were decreased at days 9 and 12 in the T0901317 treated cells compared to the DMSO control (Figure 3.13). This suggests that Lpl could potentially be a target gene of RORα in cartilage.

Figure 3.13 Lpl Protein Levels Appear Decreased at Days 9 and 12 in Micromass Cultures with Treatment of RORα Inverse Agonist

Mesenchymal cells were dissected from forelimbs and hindlimbs of E11.5 CD1 mouse embryos. The cells were isolated, cultured, and grown in micromass cultures for 12 days. Micromasses were treated with either DMSO vehicle or 20 μM T0901317. Total protein was isolated by incubating cells in RIPA lysis buffer. Protein levels were analyzed using western blot. Lpl protein levels appeared to be decreased at day 9 and 12 in the T0901317 treated cells compared to the DMSO control. Data shown are representative from 3 independent trials.

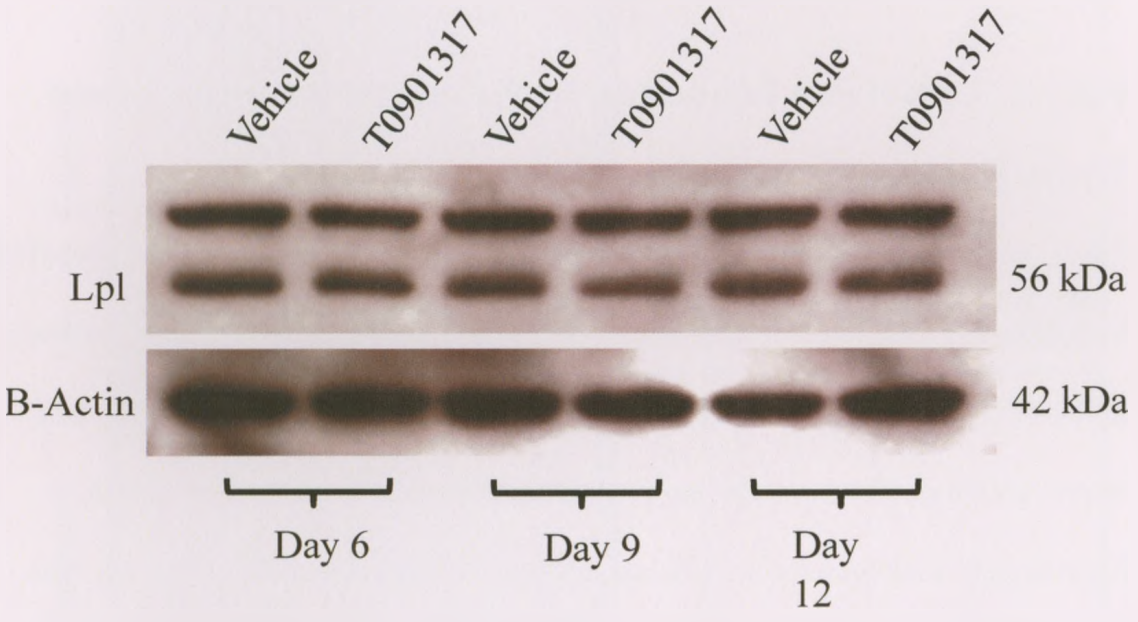
Vehicle
T0901317
Vehicle
T0901317
Vehicle
T0901317
Lpl
56 kDa
B-Actin
42 kDa
Day 6
Day 9
Day 12

Figure 3.14 Lpl Protein Expression is Decreased in RORα Inverse Agonist Treated Bones

Tibiae were isolated from E15.5 mouse embryos. Tissues were fixed and prepared for histology. Immunohistochemistry was performed with a Lpl primary antibody followed by secondary antibody and visualization with the substrate DAB (dark brown staining). Extracellular matrix was counterstained with methyl green. Representative images show evidence that growth plates from tibiae treated with T0901317 have less Lpl protein expression than the control sections. Data shown are representative from 3 independent trials.

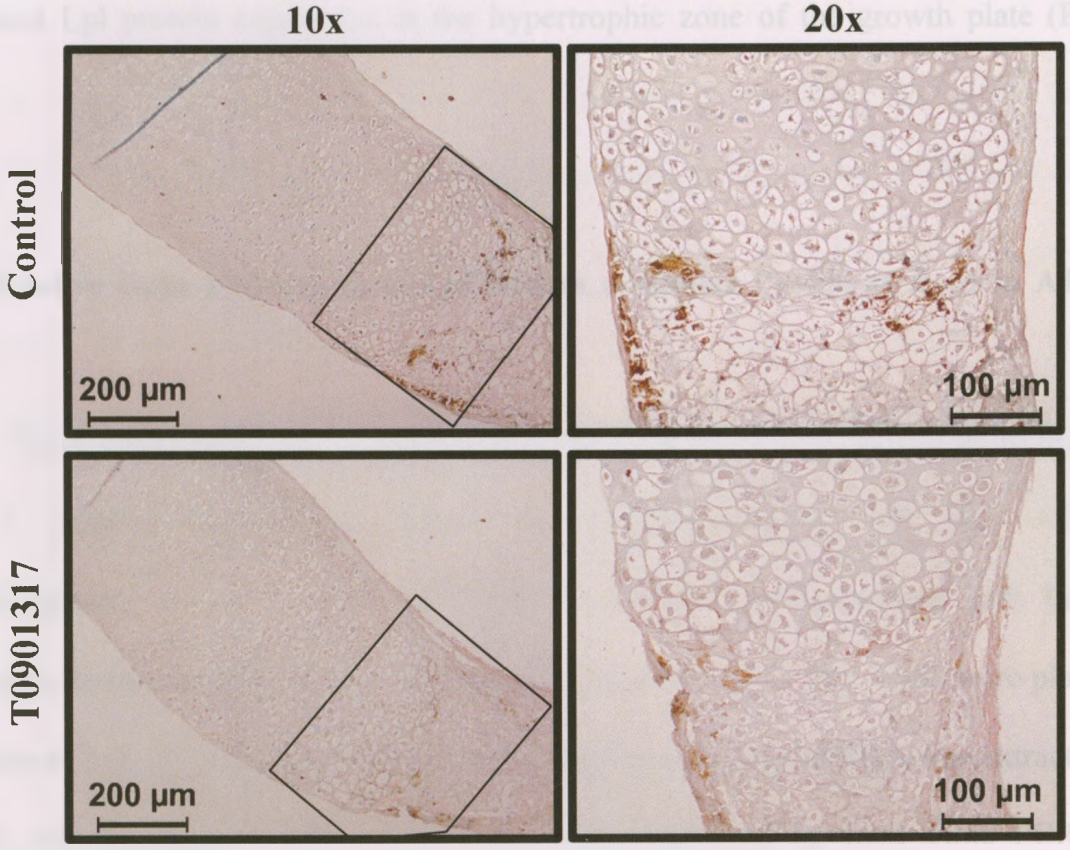
10x
20x
Control
T0901317
200 µm
100 µm
200 µm
100 µm

3.11 Lpl Protein Expression is Decreased in RORα Inverse Agonist Treated Bones

After I found that Lpl gene expression was decreased in RORα inverse agonist treated micromass cultures, I wanted to go back and analyze protein expression in the tibia organ culture system previously described. In the DMSO control bones, there was staining for Lpl in the hypertrophic zone (Figure 3.14). T0901317 treatment caused decreased Lpl protein expression in the hypertrophic zone of the growth plate (Figure 3.14).

3.12 Relative Gene Expression of *Lpl* follows a Similar Profile as *Rorα* in ATDC5 cells

Next, I was interested in determining the gene expression profile of RORα and Lpl, a putative downstream target, the pre-chondrogenic cell line ATDC5. Chondrogenesis can be induced in ATDC5 cells by supplementation with Insulin-transferrin-sodium selenite media (Shukunami, Shigeno et al. 1996). Cells were plated at a density of 5 X 10^4 cells per well in six-well culture plates. Total RNA was extracted on days 5, 10, 15 and 20 and mRNA levels were quantified by Real Time PCR. In agreement with the observation that RORα is upregulated with chondrocyte hypertrophy (Woods, James et al. 2009), there was an increase in RORα gene expression at day 15 of culture (Figure 3.15A). I then wanted to determine the expression profile of *Lpl* and if peak expression of *Lpl* followed RORα as predicted. Accordingly, *Lpl* gene expression was maximally expressed at day 20 of culture (Figure 3.15B). This supports the model that *Lpl* is downstream of RORα.

3.13 Expression of *Lpl* is Decreased upon Overexpression of RORα in Transfected ATDC5 Cells

All studies previously performed in this thesis analyzed the effect of inhibition of RORα on lipid metabolism. As such, I wanted to observe the effect of a gain-in-function in RORα on putative downstream targets, specifically Lpl. I generated a cell line of stable transfectants that were transfected with a mouse RORα cDNA clone. I isolated RNA on days 3, 6, 9, and 12 and quantified using Real Time PCR. To confirm that the transfections were successful, I wanted to analyze the gene expression profile of RORα in the stable transfectants. As expected, *Rorα* gene expression was significantly increased in the transfected cells compared to the control (Figure 3.16A). I anticipated that, in agreement with previous data explained in this thesis, overexpression of RORα would cause the gene expression of *Lpl* to increase; however, this was not the case. Unexpectedly, *Lpl* gene expression decreased in the transfected cells (Figure 3.16B).

3.14 Expression of Hypertrophic Differentiation Markers is Decreased upon Overexpression of RORα in Transfected ATDC5 Cells

Continuing with the analysis RORα overexpression, I proceeded to study gene expression of markers of chondrocyte hypertrophy. Employing the ATDC5 cell line of RORα stable transfectants, I isolated RNA on days 3, 6, 9 and 12 and quantified gene expression using real-time PCR. I analyzed the relative gene expression of *Runx2* and alkaline phosphatase. In agreement with previous data, overexpression of RORα resulted in an increase in relative gene expression of both markers of hypertrophic chondrocyte differentiation (Figure 3.17).

Figure 3.15 Relative Gene Expression of *Lpl* follows a Similar Profile as *RORα* in ATDC5 cells

ATDC5 cells were plated at a density of 5 X 10^4 cells/well and cultured for a period of 20 days. Total RNA was extracted on days 5, 10, 15, and 20. RNA was quantified by Real Time PCR. All relative gene expression levels were compared to house keeping gene *Gapdh* transcript levels. A) Relative *RORα* gene expression was greatest at day 15 of culture. B) The gene expression profile of *Lpl* was similar to *RORα* with peak expression at day 20 of culture. n=3, $p<0.05$.

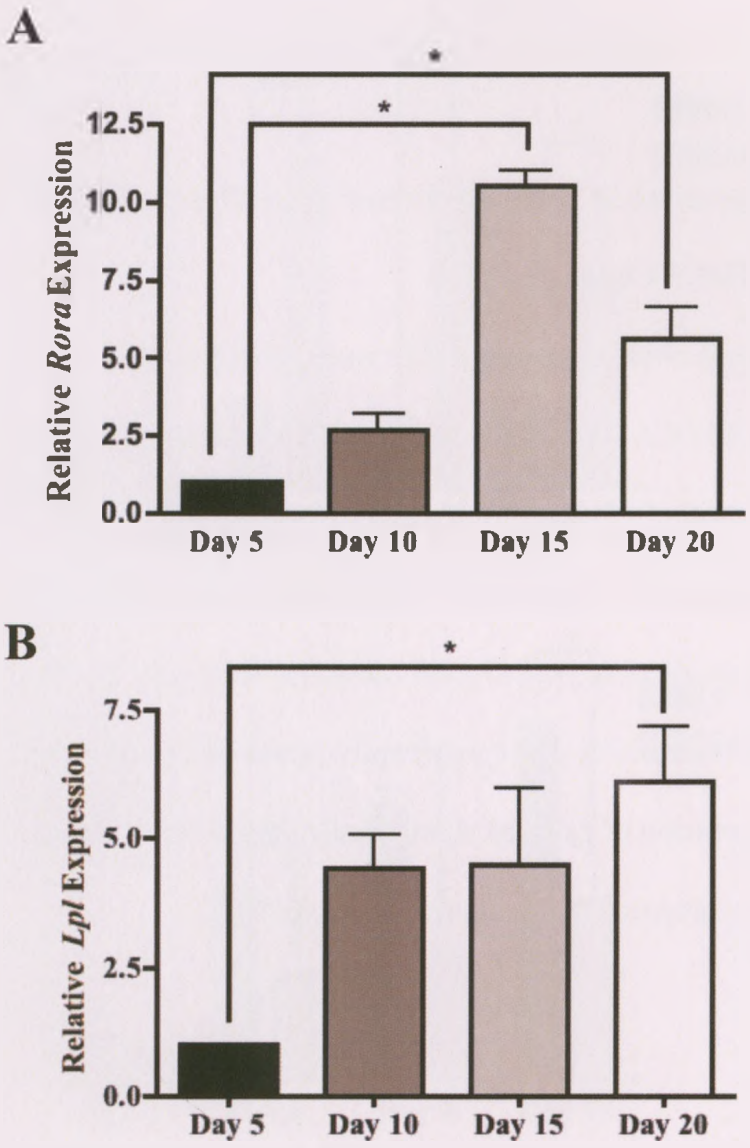
A
*
*
12.5
10.0
7.5
5.0
2.5
0.0
Relative Rora Expression
Day 5
Day 10
Day 15
Day 20
B
*
7.5
5.0
2.5
0.0
Relative Lpl Expression
Day 5
Day 10
Day 15
Day 20

Figure 3.16 Expression of *Lpl* is Decreased upon Overexpression of RORα in Transfected ATDC5 Cells

Stable transfectants overexpressing *RORα* were generated using a mouse RORα cDNA clone in ATDC5 cells. Cells were plated at a density of 5 $X10^4$ cells/well and cultured for a period of 12 days. RNA was isolated on days 3, 6, 9, and 12. RNA was quantified using Real Time PCR. All relative gene expression levels were compared to house keeping gene *Gapdh* transcript levels. A) Relative gene expression of *RORα* in transfected cells was significantly increased compared to their controls. B) The gene expression of *Lpl* was significantly decreased on days 6, 9, and 12 in the transfected cells compared to the controls. $n=3$, $p<0.05$.

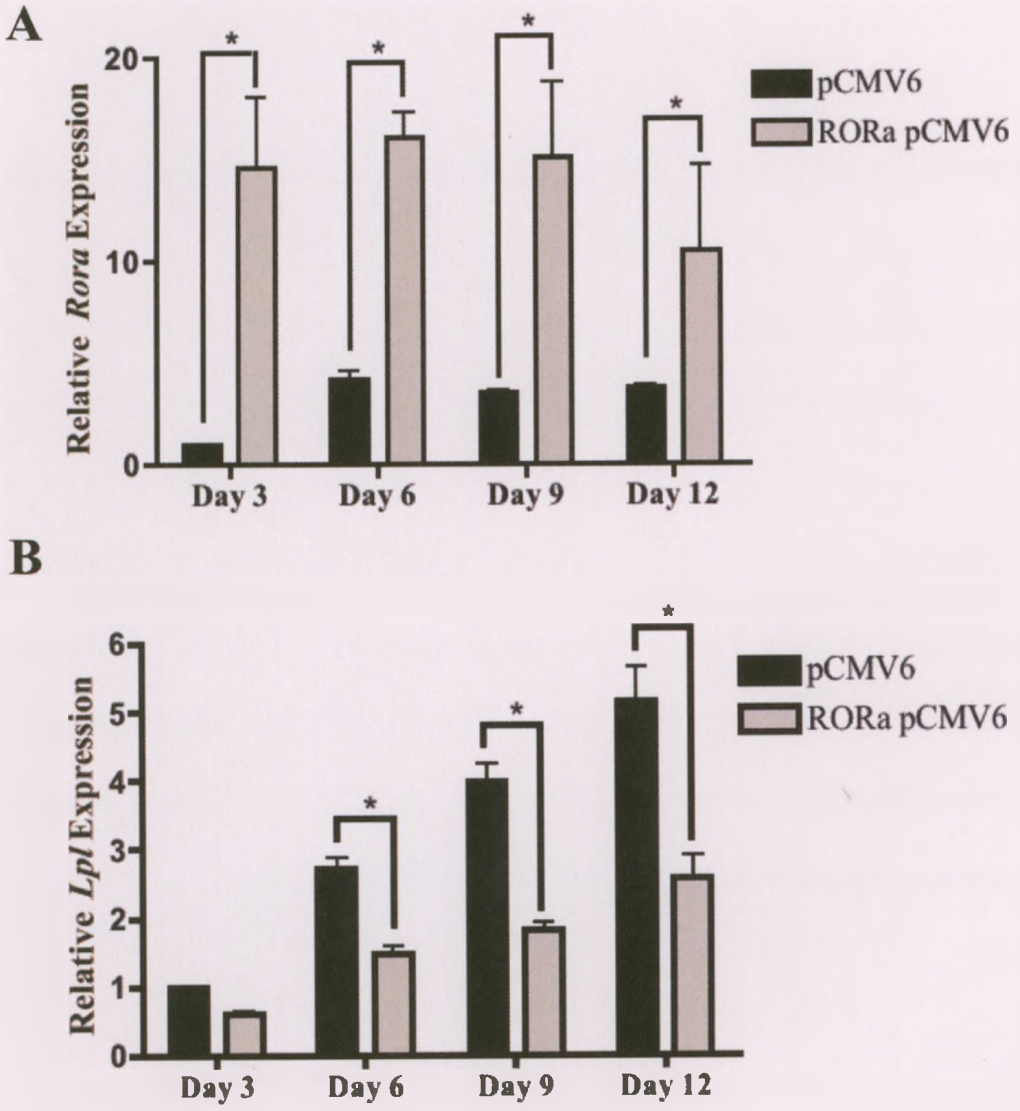
A
Relative Rora Expression
20
10
0
*
*
*
*
Day 3
Day 6
Day 9
Day 12
pCMV6
RORa pCMV6
B
Relative Lpl Expression
6
5
4
3
2
1
0
*
*
*
Day 3
Day 6
Day 9
Day 12
pCMV6
RORa pCMV6

Figure 3.17 Expression of Hypertrophic Differentiation Markers is Decreased upon Overexpression of RORα Transfected ATDC5 Cells

Stable transfectants overexpressing *RORα* were generated using a mouse RORα cDNA clone in ATDC5 cells. Cells were plated at a density of 5 $X10^4$ cells/well and cultured for a period of 12 days. RNA was isolated on days 3, 6, 9, and 12. RNA was quantified using Real Time PCR. All relative gene expression levels were compared to house keeping gene *Gapdh* transcript levels. A) Relative gene expression of alkaline phosphatase in transfected cells was significantly increased compared to their controls at day 12. B) The gene expression of *Mmp13* was significantly increased on days 6, 9, and 12 in the transfected cells compared to the controls. n=3, $p<0.05$.

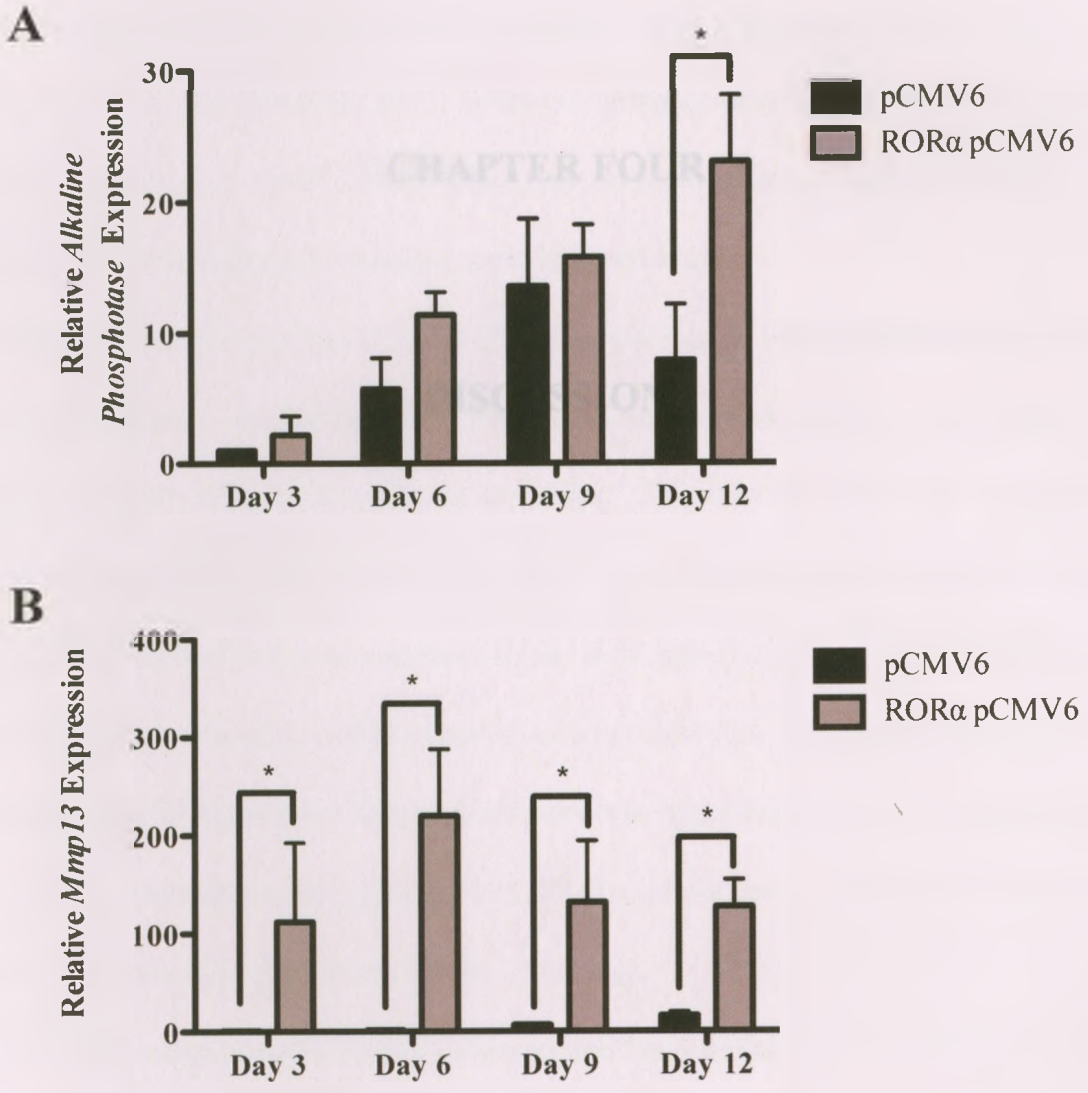
A
Relative Alkaline Phosphotase Expression
30
20
10
0
Day 3
Day 6
Day 9
Day 12
*
pCMV6
RORα pCMV6
B
Relative Mmp13 Expression
400
300
200
100
0
Day 3
Day 6
Day 9
Day 12
*
pCMV6
RORα pCMV6

CHAPTER FOUR

DISCUSSION

4.1 Summary of Results

The role of nuclear receptors in endochondral ossification is becoming increasingly complex. To date, several nuclear receptors have been recognized as being involved in chondrocyte differentiation, such as the vitamin D receptor, the thyroid hormone receptors, the peroxisome proliferator-activated receptor gamma, and the retinoic acid receptors (Miura, Tanaka et al. 2002; Weston, Hoffman et al. 2003; Bouillon, Carmeliet et al. 2008; Stanton, Li et al. 2010). The body of knowledge of RORα however, has not extended to the same degree to chondrocyte differentiation.

It has previously been found that RORα plays a role in bone metabolism *in vitro* and *in vivo* by directly modulating the expression of a bone matrix component, bone sialoprotein (BSP) (Meyer, Kneissel et al. 2000). This was the first study to address the role of RORα in the skeletal system. Recently, it has been found that staggerer (Sg) mice (which have a loss-of-function mutation in the *Rora* gene) display slower skeletal growth and delayed hypertrophic differentiation of chondrocytes (Tacchino et al., in prep). Moreover, three independent models of chondrocyte hypertrophy show an upregulation of RORα gene expression, suggesting that RORα could be a marker of chondrocyte hypertrophy (Woods, James et al. 2009).

The relationship between RORα function and lipid metabolism has been investigated in skeletal muscle where RORα regulates expression of genes involved in lipid absorption, β-oxidation, cholesterol efflux, and energy expenditure in this tissue (Lau, Nixon et al. 2004). Lastly, the role of lipid metabolism in endochondral ossification is just emerging. Studies from our laboratory have shown that during differentiation, chondrocytes increase expression of *Lpl* and *Fabp4* (Stanton, Li et al. 2010). Cholesterol, a ligand for RORα, has been shown to promote endochondral bone growth and

chondrocyte hypertrophy *in vitro* and to stimulate the expression of lipid metabolism genes (Woods, James et al. 2009). Thus, I hypothesized that RORα promotes expression of lipid metabolism genes during chondrocyte differentiation.

To study the role of RORα on chondrocyte differentiation *in vitro* I used a RORα pharmacological inverse agonist T0901317. T0901317 has been extensively used as an LXR agonist however, it was more recently found that T0901317 directly binds to RORα, resulting in the receptor's ability to interact with transcriptional co-activator proteins (Kumar, Solt et al. 2010).

My first aim was targeted at examining the effect of T0901317 treatment on bone growth. Analysis of organ culture tibiae treated with 20 μM T0901317 showed a reduction in total bone growth. Histological staining by SafraninO/Fast green of the tibiae treated with 20 μM T0901317 showed a shortened hypertrophic zone. Next I wanted to investigate the mechanism that caused the reduction in total bone growth. Through immunohistochemistry, I observed a reduction in p57 staining in the prehypertrophic zone of T0901317 treated tibiae, indicating a delay in cell cycle exit. To elucidate the role of RORα in chondrocyte differentiation, I analyzed markers of early and late differentiation in micromass cultures. Markers of early chondrocyte differentiation such as alcian blue staining, *Col2a1* expression, and *Sox9* expression were decreased with RORα inhibition. Markers of chondrocyte hypertrophy and terminal differentiation such as alkaline phosphatase activity, von Kossa staining, *Runx2* expression, and *Mmp13* expression were also decreased with T0901317 treatment, suggesting that RORα inhibition results in a reduction of all phases of chondrocyte differentiation.

I next investigated the influence of RORα inhibition on lipid metabolism genes. In the micromass cultures, RORα gene expression increased with chondrocyte differentiation with peak expression at day 9 of culture. The gene expression of all lipid metabolism genes analyzed increased with chondrocyte differentiation, with the exception of *Fabp3*. More importantly, expression of *Lpl*, a gene already found to be a direct target of RORα in other tissues (Lau, Nixon et al. 2004), peaked at day 12 of culture in control conditions, and was increased at day 6 and reduced at day 12 in the T0901317 treated cultures. In contrast, expression of *Lipg* was increased at days 9 and 12 with T0901317 treatment. There is also a decreasing trend at every time point of *Pdk4* expression with RORα inhibition. Protein levels were also examined in the T0901317 treated micromass cultures. There appears to be a moderate decrease in Lpl protein levels at days 9 and 12 in the T0901317 treated cultures. Furthermore, in the tibia organ culture system previously discussed, I found that treatment with T0901317 resulted in a reduction of Lpl protein expression in the hypertrophic zone.

All studies performed to this point analyzed the effect of the inhibition of RORα on chondrocyte differentiation and lipid metabolism. I wanted to explore the effects of a gain-of-function of RORα on these physiological processes. Unexpectedly, stable ovexpression of RORα in ATDC5 cells surprisingly resulted in a decrease in *Lpl* gene expression.

4.2 Contribution and Significant Findings

4.2.1 Contribution to the Current State of Knowledge of RORα in Chondrocyte Differentiation

Since their discovery in 1995, staggerer (Sg) mice have been thoroughly characterized. Much of this research has focused on the cerebellar phenotype of Sg mice as it has been found that Purkinje cell development in the cerebellum of Sg mice is originally normal but these cells are not able to differentiate and subsequently die (Vogel, Sinclair et al. 2000). RORα has also been linked to skeletal development. It was found that Sg mice display a bone phenotype, having thinner long bones and decreased bone mineral density leading to their characterization as osteopenic (Meyer, Kneissel et al. 2000). Recent studies have investigated the role of RORα in cartilage development using Sg mice as an *in vivo* model of RORα deficiency (Tacchino et al., in prep). Moreover, it has also been found that in three independent models of chondrocyte hypertrophy, *Rorα* expression was upregulated (Woods, James et al. 2009). However, the molecular targets of RORα in cartilage development have not been elucidated.

The phenotype of the Sg mouse however, is not limited to the cerebellum, bone, and cartilage. These mice also display multiple lipid metabolism defects such as lower levels of plasma cholesterol, HDL, and triglycerides (Hamilton, Frankel et al. 1996). Based on these findings, it was suggested that RORα also plays a role in lipid metabolism. It has been recognized that chondrocytes contain lipid droplets (Kirkpatrick, Mohr et al. 1982). Previous research in our lab has shown that there is also a connection between the nuclear receptor PPARγ2 and chondrocyte lipid metabolism (Stanton, Li et al. 2010). During differentiation chondrocytes increase expression of *Lpl* and *Fapb4* and

this increase is accompanied by an increase in *PPARγ2* expression (Stanton, Li et al. 2010). Another study from our lab has proven that cholesterol, the ligand for RORα, promotes endochondral ossification, chondrocyte hypertrophy *in vitro* and stimulates the expression of lipid metabolism genes such as *Fabp4*, *Lpl,* and *Pdk4* (Woods, James et al. 2009). The present study however, is the first *in vitro* approach using pharmacological agents to elucidate the mechanism of action of RORα on lipid metabolism genes during chondrocyte differentiation.

There is a strong body of knowledge concerning the role of nuclear receptor function in endochondral ossification. For example, the vitamin D receptor functions to regulate vascular invasion and matrix mineralization (Bouillon, Carmeliet et al. 2008). In addition to lipid metabolism, PPARγ2 functions to inhibit terminal differentiation and apoptosis (Stanton, Li et al. 2010). Retinoic acid receptors are known as major regulators of chondrocyte hypertrophy and mineralization (Weston, Hoffman et al. 2003). It is evident that nuclear receptors play an integral role in cartilage physiology.

I show for the first time the effect of the RORα inverse agonist T0901317 on chondrocyte differentiation. The observations presented in this study suggest that RORα plays a major role in chondrocyte hypertrophy. I observed a thirty-three percent reduction in the hypertrophic zone of organ culture growth plates treated with a RORα inverse agonist, a decrease in alkaline phosphatase staining and a decrease in hypertrophic markers in micromass cultures. The observed decrease in hypertrophic zone length and molecular markers could be a result of two different mechanisms. If terminal differentiation is accelerated, hypertrophic chondrocytes could potentially undergo apoptosis at a faster rate, thereby leaving less of a hypertrophic pool of cells. On the other hand, a delay in cell cycle exit by proliferating chondrocytes would also produce a

reduced hypertrophic zone. It should be noted that these possibilities are not mutually exclusive, and either or both can contribute to the observed effects of T0901317. The observed reduction in p57 staining in T0901317 treated tibiae supports the latter theory and suggests that treatment with T0901317 results in a delay in chondrocyte differentiation; a finding that directly correlates with the *in vivo* analysis of Sg mice (Tacchino et al, in prep). Furthermore, this data relates to previous literature, as RORα is known to be a regulator of differentiation in a variety of tissues. In the cerebellum of Sg mice, purkinje cells were not able to undergo differentiation (Vogel, Sinclair et al. 2000) and in muscle tissue, RORα is important in the differentiation of myotubules (Lau, Fitzsimmons et al. 2011).

4.2.2 Contribution to the Current State of Knowledge of RORα and Lipid Metabolism During Endochondral Ossification

Previous studies have discovered a connection between nuclear receptors involved in chondrocyte differentiation and lipid metabolism (Stanton, Li et al. 2010). Furthermore, literature has implicated a common link between crucial signaling pathways involved in chondrocyte differentiation such as the PI3K/AKT signaling pathway and lipid metabolism pathways such as cholesterol (Ulici, James et al. 2010). In this study, I identified a role of the nuclear orphan receptor RORα in the regulation of lipid metabolism genes in chondrocytes. Drawing a parallel with previous research, this study identified a connection between RORα and Lpl, a known target of RORα in muscle tissue (Lau, Nixon et al. 2004). Although no direct relationship could be proven, the decrease in *Lpl* expression observed with T0901317 treatment agrees with the literature to this point.

To solidify this argument, overexpression of RORα should be accompanied by an increase in *Lpl* expression. Surprisingly, I did not observe the anticipated increase in *Lpl* expression. Instead, RORα overexpression yielded a decrease in *Lpl* expression. Nuclear receptor function is very convoluted. In several instances, crosstalk between nuclear receptor pathways involves competition between receptors binding to the same response element (Jetten, Kurebayashi et al. 2001). This relationship has been demonstrated between RORs and other nuclear receptors such as Rev-Erbα and Rev-Erbβ, which act as transcriptional repressors. There is no evidence for such a mechanism in this instance. A more appropriate model is the inherent ability of numerous nuclear receptors to recruit repressors to inhibit transcription. Typically, corepressors interact with unliganded forms of nuclear receptors. The retinoic acid receptors, which are the most similar receptors to RORα, have been found to recruit co-repressor proteins in the absence of retinoic acid, thereby maintaining chromatin in the condensed state that causes transcriptional repression (Weston, Hoffman et al. 2003). Because there was an exponential increase in exogenous RORα in the transfected cells accompanied by unaltered levels of cholesterol, it is reasonable to predict that many of the receptors remained in this unliganded state, thereby hindering transcription of target genes.

Other surprising observations made were the increases in *Lpl* expression at day 6 and *Lipg* expression at days 9 and 12 in T0901317 treated micromass cultures. Both genes have been identified as targets of another nuclear receptor, LXR (Lau, Nixon et al. 2004; Norata, Ongari et al. 2005). In addition to acting as a RORα inverse agonist, T0901317 acts as a LXR agonist. Therefore, these unexpected results could potentially be due to the supplementary agonistic effects of T0901317 on LXR signaling. In this

manner, because RORα expression does not peak until approximately day 9 of culture, the increase of *Lpl* could be due to the activation of LXR.

4.3 Limitations of Research and Future Directions

In the studies present, three different *in vitro* culture systems were used. In the micromass cultures, mesenchymal cells were isolated from E11.5 mouse limb buds and cultured under pro-chondrogenic conditions. They were plated at very high densities to promote cell-cell interactions and supplemented with ascorbic acid and β-glycerophosphate (Weston, Rosen et al. 2000; James, Appleton et al. 2005; Stanton and Beier 2007). Mesenchymal cells however, are pluripotent and thus have the ability to differentiate into any mesoderm tissue such as adipose tissue, muscle tissue, bone and cartilage (Zelzer, McLean et al. 2002). Previous studies from our lab have found a decrease in gene expression of markers of other cell types accompanied by an increase of cartilage specific markers (James, Appleton et al. 2005). Because some of the cells on the periphery of the micromasses are more fibroblastic in shape, there is still the potential for cell types other than chondrocytes to be present (James, Appleton et al. 2005).

Another cell culture system used in this study was the pre-chondrogenic cell line ATDC5. Although the ATCD5 cell system resembles that of primary chondrocytes, there could be differences in gene expression between these cells and actual chondrocytes. This serves to be a limitation of this cell line and cell lines in general.

To analyze growth plate morphology, I used a tibia organ culture system. In this model, tibiae are cultured in serum free media to allow for bone growth without any endocrine functioning. Pharmacological agents can be used in this system to elucidate

specific effects in a three-dimensional context. This system provides the opportunity to study the effects of a single hormone, growth factor, or in this case, nuclear receptor. It also allows for observations to be made based on bone-specific effects. Furthermore, in the organ culture system I was able to observe changes in specific growth plate zones, a feature that is not possible in cell culture systems. However, it should be noted that not all aspects controlling cartilage development (e.g. biomechanical loads and oxygen tension) are recapitulated in this model.

In this study, the pharmacological inverse agonist T0901317 was used to study the role of RORα. This synthetic ligand binds to RORα, thereby limiting its ability to interact with co-activator proteins. On other hand, the effects of T0901317 are not specific to RORα, a factor that cannot be ignored. T0901317 was originally used as a LXR agonist (Michael, Schkeryantz et al. 2005). LXR is classically known as a key regulator of cholesterol homeostasis and therefore I cannot exclude that some of the observed effects of T0901317 on chondrocyte differentiation could be due to activation of proteins in the LXR pathway. The use of a RORα specific pharmacological agent in the *in vitro* studies discussed in this thesis would be an ideal method to alleviate the activation of other related nuclear receptors. Although it is not commercially available yet, a potential agent that would fit this criterion is the synthetic agonist SR1078. This agent functions as a RORα specific agonist and in fact, activates the receptor beyond its physiological level (Wang, Kumar et al. 2010). Another approach to identify RORα-specific effects of T0901317 was to compare drug effects to those of RORα-specific shRNAS. I attempted this approach using stable transfection of ATDC5 cells with shRNA-overexpressing plasmids, but was not able to achieve efficient knockdown of *Rora* transcript levels and correspondingly no effects on *Lpl* expression were observed (Suppl. Fig. 1).

All experiments performed in this thesis attempted to describe the role of RORα in chondrocyte differentiation through the activation of lipid metabolism genes *in vitro*. To date, the best-characterized model of RORα investigations *in vivo* is the Sg mouse. This mutant however, has intrinsic complications in that skeletal phenotypes detected could be due to endocrine limitations and mechanical restraints of the mice themselves. To control for these external factors, a cartilage-specific knockout mouse of RORα would be ideal and would also help to overcome the limitations of the *in vitro* culture systems described above. For this to be performed, a mouse with a floxed *Rora* allele crossed with a mouse expressing Cre recombinase under the control of a collagen II promoter would remove RORα from cartilage tissue only. Our lab has developed tissue-specific knockdowns for a variety of other genes such as *Gsk3b*, *Atrx,* and *Rac1* (Wang, Woods et al. 2007; Solomon, Li et al. 2009; Ulici, Hoenselaar et al. 2009; Gillespie, Ulici et al. 2011).

Analyzing gene expression and protein profiles of potential down stream targets are valuable methods in identifying the roles of nuclear receptors during chondrocyte differentiation. To fully understand RORa's role in cartilage physiology, direct or indirect effects of this transcription factors need to be distinguished. Quantitative chromatic immunoprecipitation (ChIP) assays would allow for the identification of direct downstream targets of RORα. This would further allow us to identify the molecular basis of any changes observed in the cell culture or organ culture experiments. There are commercially available antibodies against RORα that have been previously used for ChIP from mouse tissues (Fujieda, Bremner et al. 2009). However, in our experience they are not specific in Western blotting, which raises questions about their suitability for ChIP. Furthermore, ChIP should ideally be performed on primary chondrocytes but we are limited by our ability extract enough cells for ChIP. Rather, the stable transfectant

ATDC5 cell line that has been produced which overexpresses the RORα gene could be applied. The myc tag on the overexpressed RORα could also be used for ChIP as this antibody has been used for a variety of experiments (Nateri, Spencer-Dene et al. 2005). One caveat of this approach is that approximately ten-fold overexpression of this transcription factor as observed in my study could yield non-physiological binding events.

4.4 Significance

The studies in this thesis have shown that T0901317 treatment affects chondrocyte differentiation, in particular chondrocyte hypertrophy. My thesis suggests RORα to be an important regulator of late chondrocyte differentiation, potentially through the regulation of lipid metabolism genes such as *Lpl, Pdk4,* and *Lipg.* The search for potential nuclear receptors and their effect on the regulatory pathways of chondrocyte differentiation remains a challenging task. I have however, contributed to this field by suggesting that RORα plays an integral role in chondrocyte differentiation. Ultimately, my studies have contributed valuable insights into chondrocyte physiology during skeletal development and potentially the pathogenesis skeletal diseases. The studies performed here contribute to improved understanding of complex molecular pathways that occur during bone development and will hopefully lead to improved treatments of skeletal malformations. Finally, due to the fact that OA articular chondrocytes undergo hypertrophy (Aigner, Kurz et al. 2002), RORα could be implicated as a potential therapeutic target since inhibition of the receptor results in delayed hypertrophic differentiation. Targeting RORα in OA therapy is not unreasonable as nuclear receptors are increasingly being investigated as potential targets to prevent or slow the progression of the disease (Loeser 2009).

REFERENCES

Agoston, H., S. Khan, et al. (2007). "C-type natriuretic peptide regulates endochondral bone growth through p38 MAP kinase-dependent and -independent pathways." BMC developmental biology **7**: 18.

Ahrens, P. B., M. Solursh, et al. (1977). "Stage-related capacity for limb chondrogenesis in cell culture." Developmental biology **60**(1): 69-82.

Aigner, T., B. Kurz, et al. (2002). "Roles of chondrocytes in the pathogenesis of osteoarthritis." Current opinion in rheumatology **14**(5): 578-584.

Aigner, T., A. Sachse, et al. (2006). "Osteoarthritis: pathobiology-targets and ways for therapeutic intervention." Advanced drug delivery reviews **58**(2): 128-149.

Akiyama, H., M. C. Chaboissier, et al. (2002). "The transcription factor Sox9 has essential roles in successive steps of the chondrocyte differentiation pathway and is required for expression of Sox5 and Sox6." Genes & development **16**(21): 2813-2828.

Appleton, C. T., V. Pitelka, et al. (2007). "Global analyses of gene expression in early experimental osteoarthritis." Arthritis and rheumatism **56**(6): 1854-1868.

Atkins, G. B., X. Hu, et al. (1999). "Coactivators for the orphan nuclear receptor RORalpha." Molecular endocrinology **13**(9): 1550-1557.

Ballock, R. T. and R. J. O'Keefe (2003). "Physiology and pathophysiology of the growth plate." Birth defects research. Part C, Embryo today : reviews **69**(2): 123-143.

Bassett, J. H., P. J. O'Shea, et al. (2007). "Thyroid hormone excess rather than thyrotropin deficiency induces osteoporosis in hyperthyroidism." Molecular endocrinology **21**(5): 1095-1107.

Bassett, J. H. and G. R. Williams (2003). "The molecular actions of thyroid hormone in bone." Trends in endocrinology and metabolism: TEM **14**(8): 356-364.

Beier, F. (2005). "Cell-cycle control and the cartilage growth plate." Journal of cellular physiology **202**(1): 1-8.

Bitsch, F., R. Aichholz, et al. (2003). "Identification of natural ligands of retinoic acid receptor-related orphan receptor alpha ligand-binding domain expressed in Sf9 cells--a mass spectrometry approach." Analytical biochemistry **323**(1): 139-149.

Bouillon, R., G. Carmeliet, et al. (2008). "Vitamin D and human health: lessons from vitamin D receptor null mice." Endocrine reviews **29**(6): 726-776.

Buckwalter, J. A. and H. J. Mankin (1998). "Articular cartilage: degeneration and osteoarthritis, repair, regeneration, and transplantation." Instructional course lectures **47**: 487-504.

Buckwalter, J. A., J. Martin, et al. (2000). "Synovial joint degeneration and the syndrome of osteoarthritis." Instructional course lectures **49**: 481-489.

Buckwalter, J. A. and J. A. Martin (2006). "Osteoarthritis." Advanced drug delivery reviews **58**(2): 150-167.

Cash, D. E., C. B. Bock, et al. (1997). "Retinoic acid receptor alpha function in vertebrate limb skeletogenesis: a modulator of chondrogenesis." The Journal of cell biology **136**(2): 445-457.

Chen, J. D. and R. M. Evans (1995). "A transcriptional co-repressor that interacts with nuclear hormone receptors." Nature **377**(6548): 454-457.

Dreier, R. (2010). "Hypertrophic differentiation of chondrocytes in osteoarthritis: the developmental aspect of degenerative joint disorders." Arthritis research & therapy **12**(5): 216.

Erben, R. G., D. W. Soegiarto, et al. (2002). "Deletion of deoxyribonucleic acid binding domain of the vitamin D receptor abrogates genomic and nongenomic functions of vitamin D." Molecular endocrinology **16**(7): 1524-1537.

Fitzsimmons, R. L., P. Lau, et al. (2011). "Retinoid-related orphan receptor alpha and the regulation of lipid homeostasis." The Journal of steroid biochemistry and molecular biology.

Foster, H. S. (1995). "Probable impact of the 1994 elections on laboratory medicine." Clinical chemistry **41**(8 Pt 2): 1223-1227.

Foster, J. W., M. A. Dominguez-Steglich, et al. (1994). "Campomelic dysplasia and autosomal sex reversal caused by mutations in an SRY-related gene." Nature **372**(6506): 525-530.

Fu, X., W. Wang, et al. (2011). "[Progress of parathyroid hormone and parathyroid hormone-related protein on normal and osteoarthritis cartilages]." Zhongguo xiu fu chong jian wai ke za zhi = Zhongguo xiufu chongjian waike zazhi = Chinese journal of reparative and reconstructive surgery **25**(3): 299-302.

Fujieda, H., R. Bremner, et al. (2009). "Retinoic acid receptor-related orphan receptor alpha regulates a subset of cone genes during mouse retinal development." Journal of neurochemistry **108**(1): 91-101.

Gerber, H. P., T. H. Vu, et al. (1999). "VEGF couples hypertrophic cartilage remodeling, ossification and angiogenesis during endochondral bone formation." Nature medicine **5**(6): 623-628.

Ghyselinck, N. B., V. Dupe, et al. (1997). "Role of the retinoic acid receptor beta (RARbeta) during mouse development." The International journal of developmental biology **41**(3): 425-447.

Giguere, V. (1999). "Orphan nuclear receptors: from gene to function." Endocrine reviews **20**(5): 689-725.

Giguere, V., M. Tini, et al. (1994). "Isoform-specific amino-terminal domains dictate DNA-binding properties of ROR alpha, a novel family of orphan hormone nuclear receptors." Genes & development **8**(5): 538-553.

Gillespie, J. R., V. Ulici, et al. (2011). "Deletion of glycogen synthase kinase-3beta in cartilage results in up-regulation of glycogen synthase kinase-3alpha protein expression." Endocrinology **152**(5): 1755-1766.

Hamilton, B. A., W. N. Frankel, et al. (1996). "Disruption of the nuclear hormone receptor RORalpha in staggerer mice." Nature **379**(6567): 736-739.

Hojo, H., S. Ohba, et al. (2010). "Coordination of chondrogenesis and osteogenesis by hypertrophic chondrocytes in endochondral bone development." Journal of bone and mineral metabolism **28**(5): 489-502.

Horlein, A. J., A. M. Naar, et al. (1995). "Ligand-independent repression by the thyroid hormone receptor mediated by a nuclear receptor co-repressor." Nature **377**(6548): 397-404.

Houck, K. A., K. M. Borchert, et al. (2004). "T0901317 is a dual LXR/FXR agonist." Molecular genetics and metabolism **83**(1-2): 184-187.

Hunziker, E. B. (1994). "Mechanism of longitudinal bone growth and its regulation by growth plate chondrocytes." Microscopy research and technique **28**(6): 505-519.

James, C. G., C. T. Appleton, et al. (2005). "Microarray analyses of gene expression during chondrocyte differentiation identifies novel regulators of hypertrophy." Molecular biology of the cell **16**(11): 5316-5333.

Jetten, A. M., S. Kurebayashi, et al. (2001). "The ROR nuclear orphan receptor subfamily: critical regulators of multiple biological processes." Progress in nucleic acid research and molecular biology **69**: 205-247.

Kallen, J., J. M. Schlaeppi, et al. (2004). "Crystal structure of the human RORalpha Ligand binding domain in complex with cholesterol sulfate at 2.2 A." The Journal of biological chemistry **279**(14): 14033-14038.

Kallen, J. A., J. M. Schlaeppi, et al. (2002). "X-ray structure of the hRORalpha LBD at 1.63 A: structural and functional data that cholesterol or a cholesterol derivative is the natural ligand of RORalpha." Structure **10**(12): 1697-1707.

Kang, H. S., M. Angers, et al. (2007). "Gene expression profiling reveals a regulatory role for ROR alpha and ROR gamma in phase I and phase II metabolism." Physiological genomics **31**(2): 281-294.

Kelman, Z. and M. O'Donnell (1995). "Structural and functional similarities of prokaryotic and eukaryotic DNA polymerase sliding clamps." Nucleic acids research **23**(18): 3613-3620.

Kirkpatrick, C. J., W. Mohr, et al. (1982). "Alterations in articular chondrocyte growth and proteoglycan synthesis due to prostanoid precursors." Rheumatology international **2**(1): 31-34.

Kobayashi, T., U. I. Chung, et al. (2002). "PTHrP and Indian hedgehog control differentiation of growth plate chondrocytes at multiple steps." Development **129**(12): 2977-2986.

Komori, T., H. Yagi, et al. (1997). "Targeted disruption of Cbfa1 results in a complete lack of bone formation owing to maturational arrest of osteoblasts." Cell **89**(5): 755-764.

Koyama, E., E. B. Golden, et al. (1999). "Retinoid signaling is required for chondrocyte maturation and endochondral bone formation during limb skeletogenesis." Developmental biology **208**(2): 375-391.

Kronenberg, H. M. (2003). "Developmental regulation of the growth plate." Nature **423**(6937): 332-336.

Kumar, N., L. A. Solt, et al. (2010). "The benzenesulfoamide T0901317 [N-(2,2,2-trifluoroethyl)-N-[4-[2,2,2-trifluoro-1-hydroxy-1-(trifluorometh yl)ethyl]phenyl]-benzenesulfonamide] is a novel retinoic acid receptor-related orphan receptor-alpha/gamma inverse agonist." Molecular pharmacology **77**(2): 228-236.

Kumar, R. and E. B. Thompson (1999). "The structure of the nuclear hormone receptors." Steroids **64**(5): 310-319.

Lanske, B., A. C. Karaplis, et al. (1996). "PTH/PTHrP receptor in early development and Indian hedgehog-regulated bone growth." Science **273**(5275): 663-666.

Laron, Z. (2008). "Insulin-like growth factor-I treatment of children with Laron syndrome (primary growth hormone insensitivity)." Pediatric endocrinology reviews : PER **5**(3): 766-771.

Lau, P., R. L. Fitzsimmons, et al. (2011). "Homozygous staggerer (sg/sg) mice display improved insulin sensitivity and enhanced glucose uptake in skeletal muscle." Diabetologia **54**(5): 1169-1180.

Lau, P., S. J. Nixon, et al. (2004). "RORalpha regulates the expression of genes involved in lipid homeostasis in skeletal muscle cells: caveolin-3 and CPT-1 are direct targets of ROR." The Journal of biological chemistry **279**(35): 36828-36840.

Laudet, V. (1997). "Evolution of the nuclear receptor superfamily: early diversification from an ancestral orphan receptor." Journal of molecular endocrinology **19**(3): 207-226.

Lefebvre, V., P. Li, et al. (1998). "A new long form of Sox5 (L-Sox5), Sox6 and Sox9 are coexpressed in chondrogenesis and cooperatively activate the type II collagen gene." The EMBO journal **17**(19): 5718-5733.

Li, Y. C., A. E. Pirro, et al. (1997). "Targeted ablation of the vitamin D receptor: an animal model of vitamin D-dependent rickets type II with alopecia." Proceedings of the National Academy of Sciences of the United States of America **94**(18): 9831-9835.

Loeser, R. F. (2009). "Articular cartilage nuclear receptors: an emerging target for treatment of osteoarthritis." Osteoarthritis and cartilage / OARS, Osteoarthritis Research Society **17**(7): 829-831.

Lohnes, D., P. Kastner, et al. (1993). "Function of retinoic acid receptor gamma in the mouse." Cell **73**(4): 643-658.

Lufkin, T., D. Lohnes, et al. (1993). "High postnatal lethality and testis degeneration in retinoic acid receptor alpha mutant mice." Proceedings of the National Academy of Sciences of the United States of America **90**(15): 7225-7229.

Mamontova, A., S. Seguret-Mace, et al. (1998). "Severe atherosclerosis and hypoalphalipoproteinemia in the staggerer mouse, a mutant of the nuclear receptor RORalpha." Circulation **98**(24): 2738-2743.

Matsui, Y. (2010). "[Genetic basis for skeletal disease. Genetic defects in chondrodysplasia]." Clinical calcium **20**(8): 1182-1189.

Meyer, T., M. Kneissel, et al. (2000). "In vitro and in vivo evidence for orphan nuclear receptor RORalpha function in bone metabolism." Proceedings of the National Academy of Sciences of the United States of America **97**(16): 9197-9202.

Michael, L. F., J. M. Schkeryantz, et al. (2005). "The pharmacology of LXR." Mini reviews in medicinal chemistry **5**(8): 729-740.

Mitro, N., L. Vargas, et al. (2007). "T0901317 is a potent PXR ligand: implications for the biology ascribed to LXR." FEBS letters **581**(9): 1721-1726.

Miura, M., K. Tanaka, et al. (2002). "Thyroid hormones promote chondrocyte differentiation in mouse ATDC5 cells and stimulate endochondral ossification in fetal mouse tibias through iodothyronine deiodinases in the growth plate." Journal of bone and mineral research : the official journal of the American Society for Bone and Mineral Research **17**(3): 443-454.

Nateri, A. S., B. Spencer-Dene, et al. (2005). "Interaction of phosphorylated c-Jun with TCF4 regulates intestinal cancer development." Nature **437**(7056): 281-285.

Ng, L. J., S. Wheatley, et al. (1997). "SOX9 binds DNA, activates transcription, and coexpresses with type II collagen during chondrogenesis in the mouse." Developmental biology **183**(1): 108-121.

Norata, G. D., M. Ongari, et al. (2005). "Liver X receptor and retinoic X receptor agonists modulate the expression of genes involved in lipid metabolism in human endothelial cells." International journal of molecular medicine **16**(4): 717-722.

O'Keefe, R. J., J. E. Puzas, et al. (1994). "Analysis of type II and type X collagen synthesis in cultured growth plate chondrocytes by in situ hybridization: rapid induction of type X collagen in culture." Journal of bone and mineral research : the official journal of the American Society for Bone and Mineral Research **9**(11): 1713-1722.

Olsen, B. R., A. M. Reginato, et al. (2000). "Bone development." Annual review of cell and developmental biology **16**: 191-220.

Opperman, L. A. (2000). "Cranial sutures as intramembranous bone growth sites." Developmental dynamics : an official publication of the American Association of Anatomists **219**(4): 472-485.

Poole, A. R. (1999). "An introduction to the pathophysiology of osteoarthritis." Frontiers in bioscience : a journal and virtual library **4**: D662-670.

Schwartz, N. B. and M. Domowicz (2002). "Chondrodysplasias due to proteoglycan defects." Glycobiology **12**(4): 57R-68R.

Shao, Y. Y., L. Wang, et al. (2005). "Expression and activation of peroxisome proliferator-activated receptors in growth plate chondrocytes." Journal of orthopaedic research : official publication of the Orthopaedic Research Society **23**(5): 1139-1145.

Shioi, T., J. R. McMullen, et al. (2002). "Akt/protein kinase B promotes organ growth in transgenic mice." Molecular and cellular biology **22**(8): 2799-2809.

Shukunami, C., K. Ishizeki, et al. (1997). "Cellular hypertrophy and calcification of embryonal carcinoma-derived chondrogenic cell line ATDC5 in vitro." Journal of bone and mineral research : the official journal of the American Society for Bone and Mineral Research **12**(8): 1174-1188.

Shukunami, C., C. Shigeno, et al. (1996). "Chondrogenic differentiation of clonal mouse embryonic cell line ATDC5 in vitro: differentiation-dependent gene expression of parathyroid hormone (PTH)/PTH-related peptide receptor." The Journal of cell biology **133**(2): 457-468.

Solomon, L. A., J. R. Li, et al. (2009). "Loss of ATRX in chondrocytes has minimal effects on skeletal development." PloS one **4**(9): e7106.

Spranger, J. (1992). "International classification of osteochondrodysplasias. The International Working Group on Constitutional Diseases of Bone." European journal of pediatrics **151**(6): 407-415.

Spranger, J., A. Winterpacht, et al. (1994). "The type II collagenopathies: a spectrum of chondrodysplasias." European journal of pediatrics **153**(2): 56-65.

St-Jacques, B., M. Hammerschmidt, et al. (1999). "Indian hedgehog signaling regulates proliferation and differentiation of chondrocytes and is essential for bone formation." Genes & development **13**(16): 2072-2086.

Stanton, L. A. and F. Beier (2007). "Inhibition of p38 MAPK signaling in chondrocyte cultures results in enhanced osteogenic differentiation of perichondral cells." Experimental cell research **313**(1): 146-155.

Stanton, L. A., J. R. Li, et al. (2010). "PPARgamma2 expression in growth plate chondrocytes is regulated by p38 and GSK-3." Journal of cellular and molecular medicine **14**(1-2): 242-256.

Stanton, L. A., S. Sabari, et al. (2004). "p38 MAP kinase signalling is required for hypertrophic chondrocyte differentiation." The Biochemical journal **378**(Pt 1): 53-62.

Stanton, L. A., T. M. Underhill, et al. (2003). "MAP kinases in chondrocyte differentiation." Developmental biology **263**(2): 165-175.

Steinmayr, M., E. Andre, et al. (1998). "staggerer phenotype in retinoid-related orphan receptor alpha-deficient mice." Proceedings of the National Academy of Sciences of the United States of America **95**(7): 3960-3965.

Stevens, D. A., R. P. Hasserjian, et al. (2000). "Thyroid hormones regulate hypertrophic chondrocyte differentiation and expression of parathyroid hormone-related peptide and its receptor during endochondral bone formation." Journal of bone and mineral research : the official journal of the American Society for Bone and Mineral Research **15**(12): 2431-2442.

Street, J., M. Bao, et al. (2002). "Vascular endothelial growth factor stimulates bone repair by promoting angiogenesis and bone turnover." Proceedings of the National Academy of Sciences of the United States of America **99**(15): 9656-9661.

Superti-Furga, A., L. Bonafe, et al. (2001). "Molecular-pathogenetic classification of genetic disorders of the skeleton." American journal of medical genetics **106**(4): 282-293.

Ulici, V., K. D. Hoenselaar, et al. (2009). "The role of Akt1 in terminal stages of endochondral bone formation: angiogenesis and ossification." Bone **45**(6): 1133-1145.

Ulici, V., C. G. James, et al. (2010). "Regulation of gene expression by PI3K in mouse growth plate chondrocytes." PloS one **5**(1): e8866.

Vogel, M. W., M. Sinclair, et al. (2000). "Purkinje cell fate in staggerer mutants: agenesis versus cell death." Journal of neurobiology **42**(3): 323-337.

Vortkamp, A., K. Lee, et al. (1996). "Regulation of rate of cartilage differentiation by Indian hedgehog and PTH-related protein." Science **273**(5275): 613-622.

Vu-Dac, N., P. Gervois, et al. (1997). "Transcriptional regulation of apolipoprotein A-I gene expression by the nuclear receptor RORalpha." The Journal of biological chemistry **272**(36): 22401-22404.

Wang, G., A. Woods, et al. (2007). "Genetic ablation of Rac1 in cartilage results in chondrodysplasia." Developmental biology **306**(2): 612-623.

Wang, G., A. Woods, et al. (2004). "RhoA/ROCK signaling suppresses hypertrophic chondrocyte differentiation." The Journal of biological chemistry **279**(13): 13205-13214.

Wang, Y., N. Kumar, et al. (2010). "Identification of SR1078, a synthetic agonist for the orphan nuclear receptors RORalpha and RORgamma." ACS chemical biology **5**(11): 1029-1034.

Wang, Y., L. A. Solt, et al. (2010). "Regulation of FGF21 expression and secretion by retinoic acid receptor-related orphan receptor alpha." The Journal of biological chemistry **285**(21): 15668-15673.

Weston, A. D., R. A. Chandraratna, et al. (2002). "Requirement for RAR-mediated gene repression in skeletal progenitor differentiation." The Journal of cell biology **158**(1): 39-51.

Weston, A. D., L. M. Hoffman, et al. (2003). "Revisiting the role of retinoid signaling in skeletal development." Birth defects research. Part C, Embryo today : reviews **69**(2): 156-173.

Weston, A. D., V. Rosen, et al. (2000). "Regulation of skeletal progenitor differentiation by the BMP and retinoid signaling pathways." The Journal of cell biology **148**(4): 679-690.

Woods, A., C. G. James, et al. (2009). "Control of Chondrocyte Gene Expression by Actin Dynamics: A Novel Role of Cholesterol/Roralpha Signaling in Endochondral Bone Growth." Journal of cellular and molecular medicine.

Yasoda, A., H. Kitamura, et al. (2009). "Systemic administration of C-type natriuretic peptide as a novel therapeutic strategy for skeletal dysplasias." Endocrinology **150**(7): 3138-3144.

Yoshizawa, T., Y. Handa, et al. (1997). "Mice lacking the vitamin D receptor exhibit impaired bone formation, uterine hypoplasia and growth retardation after weaning." Nature genetics **16**(4): 391-396.

Zelzer, E., W. McLean, et al. (2002). "Skeletal defects in VEGF(120/120) mice reveal multiple roles for VEGF in skeletogenesis." Development **129**(8): 1893-1904.

Zhang, P., N. J. Liegeois, et al. (1997). "Altered cell differentiation and proliferation in mice lacking p57KIP2 indicates a role in Beckwith-Wiedemann syndrome." Nature **387**(6629): 151-158.

Zhao, Q., H. Eberspaecher, et al. (1997). "Parallel expression of Sox9 and Col2a1 in cells undergoing chondrogenesis." Developmental dynamics : an official publication of the American Association of Anatomists **209**(4): 377-386.

APPENDIX A

Animal Use Protocol

AUP Number: 2007-045-06 PI Name: Beier, Frank AUP Title: Regulation Of Endochondral Bone Growth By Hormones

Official Notice of Animal Use Subcommittee (AUS) Approval: Your new Animal Use Protocol (AUP) entitled "Regulation Of Endochondral Bone Growth By Hormones " has been APPROVED by the Animal Use Subcommittee of the University Council on Animal Care. This approval, although valid for four years, and is subject to annual Protocol Renewal.2007-045-06:5

1. This AUP number must be indicated when ordering animals for this project.
2. Animals for other projects may not be ordered under this AUP number.
3. Purchases of animals other than through this system must be cleared through the ACVS office. Health certificates will be required.

The holder of this Animal Use Protocol is responsible to ensure that all associated safety components (biosafety, radiation safety, general laboratory safety) comply with institutional safety standards and have received all necessary approvals. Please consult directly with your institutional safety officers.

Submitted by: Copeman, Laura on behalf of the Animal Use Subcommittee University Council on Animal Care

***The* University *of* Western Ontario**
Animal Use Subcommittee / University Council on Animal Care
Health Sciences Centre, • London, Ontario • CANADA – N6A 5C1
PH: 519-661-2111 ext. 86768 • FL 519-661-2028
Email: auspc@uwo.ca • http://www.uwo.ca/animal/website/

APPENDIX B

Supplementary Figures

Supplementary Figure 1 Expression of *RORα* in RORα sHRNA Transfected ATDC5 Cells

Stable transfects silencing *RORα* were generated using a mouse RORα cDNA clone in ATDC5 cells. Cells were plated at a density of 5 $X10^4$ cells/well and cultured for a period of 12 days. RNA was isolated on days 3, 6, 9, and 12. RNA was quantified using Real Time PCR. All relative gene expression levels were compared to house keeping gene *Gapdh* transcript levels. B) Relative gene expression of *RORα* in transfected cells was inconclusive compared to their controls. B) The gene expression of *Lpl* was inconclusive on days 6, 9, and 12 in the transfected cells compared to the controls. n=3.

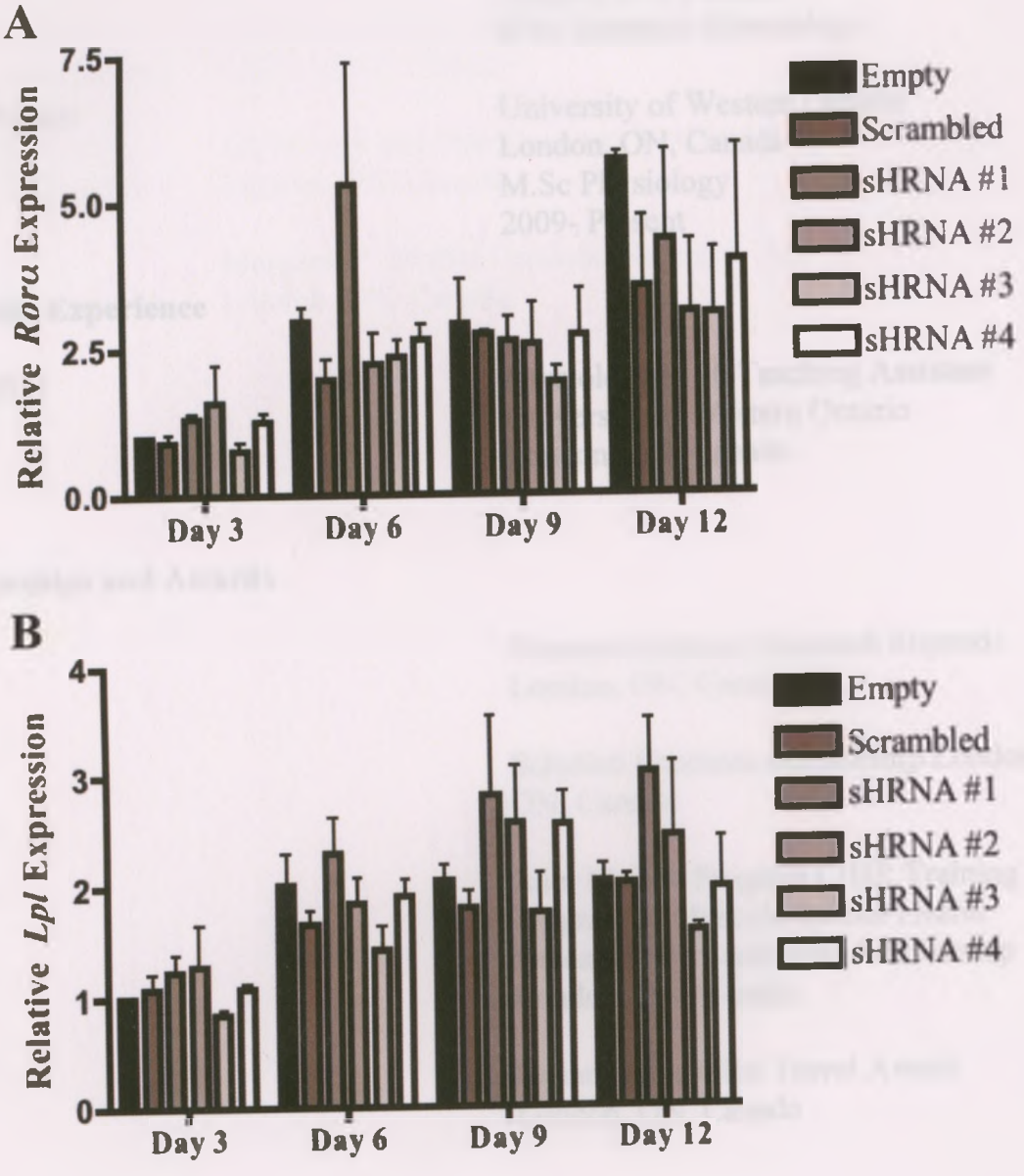
A
Relative Rora Expression
7.5
5.0
2.5
0.0
Day 3
Day 6
Day 9
Day 12
Empty
Scrambled
sHRNA #1
sHRNA #2
sHRNA #3
sHRNA #4
B
Relative Lpl Expression
4
3
2
1
0
Day 3
Day 6
Day 9
Day 12
Empty
Scrambled
sHRNA #1
sHRNA #2
sHRNA #3
sHRNA #4